

Weighted Sum-Rate Maximization for a Set of Interfering Links via Branch and Bound

Pradeep Chaturanga Weeraddana, *Student Member, IEEE*, Marian Codreanu, *Member, IEEE*,
Matti Latva-aho, *Senior Member, IEEE*, and Anthony Ephremides, *Fellow, IEEE*

Abstract—We consider the problem of weighted sum-rate maximization (WSRMax) for a set of interfering links. It plays a central role in resource allocation, link scheduling or in finding achievable rate regions for both wireline and wireless networks. This problem is known to be NP-hard. We propose a solution method, based on the branch and bound technique, which solves globally the nonconvex WSRMax problem with an optimality certificate. Efficient analytic bounding techniques are introduced and their impact on the convergence is numerically evaluated. The considered link-interference model is general enough to model a wide range of network topologies with various node capabilities, e.g., single- or multipacket transmission (or reception), simultaneous transmission and reception. Several applications, including cross-layer network utility maximization and maximum weighted link scheduling for multihop wireless networks as well as finding achievable rate regions for singlecast/multicast wireless networks, are presented. The proposed algorithm can be further used to provide other performance benchmarks by back-substituting it into any network design method which relies on WSRMax. It is also very useful for evaluating the performance loss encountered by any heuristic algorithm.

Index Terms—Branch and bound, global (nonconvex) optimization, interference, link scheduling, power and rate control, wireless networks.

I. INTRODUCTION

INTERFERENCE is inherent in wireless networks when multiple transmitters and receivers operate over a shared medium, e.g., in spatial-TDMA networks [1] or code division multiple access networks [2]. A similar kind of interference also arises in wireline networks due to electromagnetic coupling between the transmitted signals over wires which are closely bundled, e.g., in digital subscriber lines (DSL) [3]. Due to interference, the achievable rates on different links are

interdependent, i.e., the achievable rate of a particular link depends on the powers allocated to all other links. In general, this coupling makes the power and rate control problems extremely difficult to solve [4]. Among various power and rate control problems, the *weighted sum-rate maximization* (WSRMax) for an arbitrary set of interfering links plays the central role in many network control and optimization methods.

In [5]–[16], the power and rate control problem for DSL networks has been formulated as a WSRMax over the achievable rate region. Maximum weighted link scheduling for multihop wireless networks [17]–[26] is another important context in which the problem of WSRMax is directly used. Note that, for networks with fixed link capacities, the maximum weighted link scheduling problem reduces to the classical maximum weighted matching problem and can be solved in polynomial time [22], [26], [27]. However, no solution is known for the general case when the link rates depend on the power allocation of all other links. WSRMax is also encountered in various cross-layer control policies for wireless networks [22]–[25], [28]–[32], where it is the basis for physical layer resource allocation. WSRMax problem also comes up extensively in the network utility maximization (NUM) for wireless networks [33]–[35]. In this context, the WSRMax problem appears as a part of the Lagrange dual problem of the overall NUM problem. Power and rate control problem for multicast wireless networks can also be cast as a WSRMax problem [36]. Another application where WSRMax problem plays an important role is multiple-input multiple-output (MIMO) multiuser power control [37]–[45]. Thus, WSRMax appears to be a thorny problem in wireless/wireline network design and, certainly, deserves optimal solution methods.

Unfortunately, the general WSRMax problem is not yet amendable to a convex formulation [4] and in fact, it is NP-hard [46]. Therefore, we have to rely on global optimization approaches [47], [48] for computing an exact solution. One straightforward approach is based on exhaustive search in the variable space [5]. The main disadvantage of this approach is the prohibitively expensive computational complexity even in the case of very small problem instances. Better approach is to apply branch and bound techniques which essentially implement the exhaustive search in a clever manner [47]–[49]. Branch and bound methods based on difference of convex functions (DC) programming [47] have been proposed in [7]–[9] to solve (a subclass of) WSRMax. Though, DC programming is the core of their algorithms, it also limits the generality of their method to the problems in which the objective function cannot be expressed as a DC [47]. For example, in the case of multicast

Manuscript received October 05, 2010; revised January 12, 2011; accepted April 18, 2011. Date of publication May 10, 2011; date of current version July 13, 2011. The associate editor coordinating the review of this manuscript and approving it for publication was Dr. Milica Stojanovic. This work was supported by the Finnish Funding Agency for Technology and Innovation (Tekes), the Academy of Finland, Nokia, Nokia Siemens Networks, Elektrobit, Graduate School in Electronics, Telecommunications and Automation (GETA) Foundations, Nokia Foundation, the NSF by Grant CCF0728966 and by the U.S. Army Research Office by Grant W911NF-08-1-0238.

P. C. Weeraddana, M. Codreanu, and M. Latva-aho are with the Centre for Wireless Communications, University of Oulu, Oulu FI-90014, Finland (e-mail: chathu@ee.oulu.fi; codreanu@ee.oulu.fi; matti.latva-aho@ee.oulu.fi).

A. Ephremides is with the University of Maryland, College Park, MD 20742 USA (e-mail: etony@ece.umd.edu).

Color versions of one or more of the figures in this paper are available online at <http://ieeexplore.ieee.org>.

Digital Object Identifier 10.1109/TSP.2011.2152397

wireless networks the objective function cannot be cast as a DC, even when Shannon's formula is used to express the achievable link rates. Another branch and bound method has been used in [10] in the context of DSL bit loading, where the search space is discretized in advance. As a result of discretization, this method does not allow a complete control on the accuracy of the solution. An alternative optimal method was proposed in [12], where the WSRMax problem is cast as a generalized linear fractional program [50] and solved via a polyblock algorithm [48]. The method works well for small scale problems, but as pointed out in [48, Ch. 2, pp. 40–41] and [50, Sec. 6.3], it may show much slower convergence than branch and bound methods as the problem size increases. A special form of WSRMax problem is presented in [51, p. 78], [11] where the problem data and the constraints must obey certain properties and consequently the problem can be reduced to a convex formulation. However, these required properties correspond to very unlikely events in wireless/wireline networks and thus, the method has a very limited applicability. In the context of sub-optimal solution methods for the WSRMax problem, various heuristics can be found in [13]–[16], [22], [25], [26], [37]–[45], [52]. Among them, local optimization based on complementary geometric programming (CGP) [53]–[55] is one of the most promising solution [14], [16], [37], [40], [52].

The main contribution of this paper is to provide a branch and bound method for solving globally the general WSRMax problem for a set of interfering links. At each step, the algorithm computes upper and lower bounds for the optimal value. The algorithm terminates when the difference between the upper and the lower bounds is within a prespecified accuracy level. Efficient analytic bounding techniques are introduced and their impact on the convergence is numerically evaluated. The considered link-interference model is general enough to model a wide range of network topologies with various node capabilities, e.g., single- or multipacket transmission (or reception), simultaneous transmission and reception. In contrast to the previously proposed branch and bound based techniques [7]–[9], our method does not rely on the convertibility of the problem into a DC problem. Therefore, our proposed method applies to a broader class of WSRMax problems (e.g., WSRMax in multicast wireless networks). Moreover, the method proposed here is not restricted to WSRMax; it can also be used to maximize *any* system performance metric that can be expressed as a Lipschitz continuous and increasing function of signal to interference and noise ratio (SINR) values.

Our proposed branch and bound method shows some analogy to the one proposed in [10] in terms of the initial search domain and the basic bounding techniques. However, the two methods are fundamentally different in terms of branching techniques, as the algorithm proposed in [10] is designed specifically to search over a discrete space whilst our method is optimized for a continuous search space. We also provide improved bounding techniques which improve substantially the convergence speed of the algorithm.

Given its generality, the proposed algorithm can be adapted to address a wide range of network control and optimization problems. Performance benchmarks for various network topologies

can be obtained by back-substituting it into any network design method which relies on WSRMax. Several applications, including cross-layer network utility maximization and maximum weighted link scheduling for multihop wireless networks as well as finding achievable rate regions for singlecast/multicast wireless networks, are presented. As suboptimal but less complex algorithms are typically used in practice, our algorithm can also be used for evaluating their performance loss.

The rest of the paper is organized as follows. The system model and problem formulation are presented in Section II. In Section III we reformulate the original problem as a minimization of nonconvex problem over a convex set and the proposed branch and bound method is presented. In Section IV, various bounds and efficient methods for computing them are presented, which are central to the branch and bound method. Extension to WSRMax in multicast networks is presented in Section V. The numerical results are presented in Sections VI and VII concludes our paper.

Notations: All boldface lower case and upper case letters represent vectors and matrices respectively and calligraphy letters represent sets. The notation $[\mathbf{A}]_{p,q}$ denotes the (p, q) entry of the matrix \mathbf{A} , $\mathbb{R}_+^{m \times n}$ denotes the set of $m \times n$ real matrices with nonnegative entries. $|\mathcal{X}|$ denotes the cardinality of the set \mathcal{X} , $|x|$ denotes the absolute value of the scalar x , ∇f stands for the gradient of function f , and $\|\mathbf{x}\|_2$ denote the Euclidian norm of the vector \mathbf{x} . \mathbf{A}^T is the transpose of matrix \mathbf{A} , \mathbf{A}^{-1} is the inverse of matrix \mathbf{A} , and $\text{rank } \mathbf{A}$ is the rank of matrix \mathbf{A} . \mathbf{I} denotes the identity matrix, $\mathbf{1}$ denotes the vector with all 1 s, and \mathbf{e}_i represents the i th standard unit vector. The curled inequality symbol \succeq (and its strict form \succ) is used to denote the componentwise inequality between real matrices or vectors, i.e., if $\mathbf{A}, \mathbf{B} \in \mathbb{R}^{m \times n}$ then $\mathbf{A} \succeq \mathbf{B}$ means that $[\mathbf{A}]_{p,q} \geq [\mathbf{B}]_{p,q}$ for all $1 \leq p \leq m$ and $1 \leq q \leq n$. The superscript $(\cdot)^*$ is used to denote a solution of an optimization problem.

II. SYSTEM MODEL AND PROBLEM FORMULATION

The network considered consists of a collection of nodes which can send, receive and relay data across a set of links. The set of all nodes is denoted by \mathcal{N} and we label the nodes with the integer values $n = 1, \dots, N$. A link is represented as an ordered pair (i, j) of distinct nodes. The set of all links is denoted by \mathcal{L} and we label the links with the integer values $l = 1, \dots, L$. We define $\text{tran}(l)$ as the transmitter node of link l and $\text{rec}(l)$ as the receiver node of link l . The existence of a link $l \in \mathcal{L}$ implies that a direct transmission is possible from node $\text{tran}(l)$ to node $\text{rec}(l)$. Note that in the most general case \mathcal{L} may consist of a combination of wireless and wireline links, e.g., in the case of hybrid networks. We define $\mathcal{O}(n)$ as the set of links that are outgoing from node n and $\mathcal{I}(n)$ as the set of links that are incoming to node n . Furthermore, we denote the set of transmitter nodes by \mathcal{T} and the set of receiver nodes by \mathcal{R} , i.e., $\mathcal{T} = \{n \in \mathcal{N} | \mathcal{O}(n) \neq \emptyset\}$ and $\mathcal{R} = \{n \in \mathcal{N} | \mathcal{I}(n) \neq \emptyset\}$.

The model above covers a wide range of network topologies from very simple ones to more complicated ones as shown in Fig. 1. A particular class of network topologies is the one for which the set of transmitters \mathcal{T} and the set of receivers \mathcal{R} are disjoint and we refer to these networks as *bipartite* networks. Fig. 1(a) and (b) show two examples of bipartite networks. In

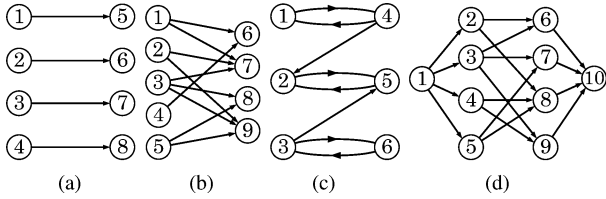


Fig. 1. Various network topologies: (a) Bipartite network, $\mathcal{T} = \{1, 2, 3, 4\}$, $\mathcal{R} = \{5, 6, 7, 8\}$, degree 1; (b) Bipartite network, $\mathcal{T} = \{1, 2, 3, 4, 5\}$, $\mathcal{R} = \{6, 7, 8, 9\}$, degree 3; (c) Nonbipartite singlehop network, $\mathcal{T} = \mathcal{R} = \{1, 2, 3, 4, 5, 6\}$, degree 3; (d) Nonbipartite multihop network, $\mathcal{T} = \{1, 2, \dots, 9\}$, $\mathcal{R} = \{2, 3, \dots, 10\}$, $\mathcal{T} \cap \mathcal{R} = \{2, 3, \dots, 9\}$, degree 4.

Fig. 1(a) each transmitter node has only one outgoing link and each receiving node has only one incoming link, i.e., $|\mathcal{O}(n)| = 1$ for all $n \in \mathcal{T}$ and $|\mathcal{I}(n)| = 1$ for all $n \in \mathcal{R}$. Borrowing terminology from the graph theory, we say this network has *degree one*.¹ In contrast, the network shown in Fig. 1(b) has degree three since all nodes $n \in \{3, 7, 9\}$ have degree 3. A network for which $\mathcal{T} \cap \mathcal{R} \neq \emptyset$ is referred to as *nonbipartite* network. Examples of nonbipartite networks are shown in Fig. 1(c) and (d). Note that all bipartite networks are necessarily singlehop networks whilst the nonbipartite networks can be either singlehop [e.g., Fig. 1(c)] or multihop [e.g., Fig. 1(d)] networks. Furthermore, all networks with degree one are necessarily bipartite and all nonbipartite networks have degrees larger than one.

In general, depending on the complexity limitations and the transceiver techniques employed at different nodes of the network, some nodes may have restricted transmit and receive capabilities. For example, certain nodes may have only singlepacket receive and/or transmit capabilities² and some nodes may not be able to transmit and receive simultaneously. These limitations create subsets of mutually exclusive links and induce a combinatorial nature for the power and rate optimization in the case of networks with degree larger than one [20], [22], [56]–[60]. An example is the maximum weighted link scheduling for multihop wireless networks [17].

We assume that all links are sharing a common channel and the interference is controlled via power allocation. We denote the channel gain from the transmitter of link i to the receiver of link j by h_{ij} . For any pair of distinct links $i \neq j$, we denote the interference coefficient from link i to link j by g_{ij} . In case of nonadjacent links (i.e., links i and j do not have common nodes), g_{ij} represents the power of the interference signal at the receiver node of link j when one unit of power is allocated to the transmitter node of link i , i.e., $g_{ij} = |h_{ij}|^2$. When links i and j are adjacent, the value of g_{ij} depends also on the transmit and receive capabilities of the common node. Specifically, we set $g_{ij} = \infty$ if links i and j are mutually exclusive and $g_{ij} = |h_{ij}|^2$ if links i and j can be simultaneously activated. Thus, $g_{ij} = g_{ji} = \infty$ for any pair of mutually exclusive links. Fig. 2 illustrates three examples of choosing the

¹In the graph theory, the degree of a vertex is the number of edges incident on it and the degree of a graph is the maximum degree of any vertex. By associating the network's nodes with vertices and the network's links with (oriented) edges, we say that the degree of node n is given by $\deg(n) = |\mathcal{I}(n)| + |\mathcal{O}(n)|$ and the degree of the network is given by $\max_{n \in \mathcal{N}} \deg(n)$.

²We say that a node has singlepacket receive capability if it can receive only from a single incoming link at a time. Similarly, we say that a node has singlepacket transmit capability if it can transmit only through a single outgoing link at a time.

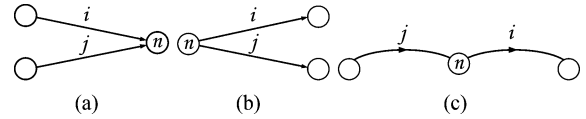


Fig. 2. Choosing the value of interference coefficient in the case of adjacent links: (a) $i, j \in \mathcal{I}(n)$, $g_{ij} = g_{ji} = \infty$ if node n has singlepacket receive capability or $g_{ij} = |h_{ii}|^2$, $g_{ji} = |h_{jj}|^2$ if node n has multipacket receive capability; (b) $i, j \in \mathcal{O}(n)$, $g_{ij} = g_{ji} = \infty$ if node n has singlepacket transmit capability or $g_{ij} = |h_{jj}|^2$, $g_{ji} = |h_{ii}|^2$ if node n has multipacket transmit capability; (c) $i \in \mathcal{O}(n)$, $j \in \mathcal{I}(n)$, $g_{ij} = g_{ji} = \infty$ if node n can not transmit and receive simultaneously or $g_{ij} = |h_{ij}|^2$ and $g_{ji} = |h_{ji}|^2$ if node n can transmit and receive simultaneously.

value of interference coefficient in the case of adjacent links. Note that in the case of nonbipartite networks, when $i \in \mathcal{O}(n)$ and $j \in \mathcal{I}(n)$, the term g_{ij} represents the power gain within the same node from its transmitter to its receiver and is referred to as the self interference coefficient [see Fig. 2(c)]. In the case of wireless networks, these gains can be several orders of magnitude larger than the power gains between distinct nodes. References [61]–[64] discuss various self-interference cancellations techniques which provides different degrees of accuracy. When such schemes are employed, g_{ij} models the residual self interference coefficient after a certain (imperfect) self interference cancellation technique was performed.

It is worthwhile to notice that the interference model described previously can be easily extended to accommodate different multiple access techniques by reinterpreting appropriately the interference coefficients. For example, in the case of wireless CDMA networks the interference coefficient g_{ij} would model the residual interference at the output of despreading filter of node $rec(j)$ [2]. Similarly, in the case wireless SDMA networks where nodes are equipped with multiple antennas, g_{ij} represents the equivalent interference coefficient measured at the output of antenna combiner of node $rec(j)$ [2]. Extensions to a multichannel scenario (e.g., FDMA or FDMA-SDMA networks) is also possible by introducing multiple links between nodes, one link for each available spectral channel and by setting $g_{ij} = 0$ if links i and j corresponds to orthogonal channels. However, all these aspects are beyond the main scope of this paper.

We consider the case where all receiver nodes are using *single-user detection* (i.e., a receiver decodes each of its intended signals by treating all other interfering signals as noise) and assume that the achievable rate of link l is given by

$$r_l = \log \left(1 + \frac{g_{ll} p_l}{\sigma^2 + \sum_{j \neq l} g_{jl} p_j} \right), \quad (1)$$

where p_l is the power allocated to link l , σ^2 represents the power of the thermal noise at the receiver and g_{ll} represent the power gain of link l , i.e., $g_{ll} = |h_{ll}|^2$. The use of Shannon formula³ for achievable rate in (1) is a common practice (see, for e.g., [2] and [3]) but it must be noted that this is not strictly correct in the case of finite length packets. However, as the packet length increases it is asymptotically correct.

³The algorithm proposed in this paper can be used for any other rate versus SINR dependence. The only restriction is that the rate must be a nondecreasing and Lipschitz continuous function of SINR.

Let us first consider the case of singlecast networks, where all links carry different information. Let β_l denote an arbitrary non-negative number which represents the weight associated with link l . Assuming that the power allocation is subject to a maximum power constraint $\sum_{l \in \mathcal{O}(n)} p_l \leq p_n^{\max}$ for each transmitter node $n \in \mathcal{T}$,⁴ the problem of weighted sum-rate maximization can be expressed as

$$\begin{aligned} & \text{maximize} && \sum_{l \in \mathcal{L}} \beta_l \log \left(1 + \frac{g_l p_l}{\sigma^2 + \sum_{j \neq l} g_{jl} p_j} \right) \\ & \text{subject to} && \sum_{l \in \mathcal{O}(n)} p_l \leq p_n^{\max}, \quad n \in \mathcal{T} \\ & && p_l \geq 0, \quad l \in \mathcal{L}, \end{aligned} \quad (2)$$

where the optimization variables are p_l for all $l \in \mathcal{L}$.

In the case of multicast networks, a transmitter can send simultaneously common information to multiple receiver nodes. We consider the general case where each transmitter node can have several multicast transmissions. Thus, for each $n \in \mathcal{T}$ we partition $\mathcal{O}(n)$ into M_n disjoint subsets of links, i.e., $\mathcal{O}(n) = \cup_{m=1}^{M_n} \mathcal{O}^m(n)$ where M_n is the number of multicast transmissions from node n and the set $\mathcal{O}^m(n)$ contains all links associated with m th multicast transmission of node n (see Fig. 3). Let p_n^m and β_n^m be the power and the nonnegative weight allocated to m th multicast transmission of node n . By noting that the maximum rate achievable by all links in $\mathcal{O}^m(n)$ is given by $r_n^m = \min_{l \in \mathcal{O}^m(n)} r_l$, the weighted sum-rate maximization problem can be expressed as (3) at the bottom of the page, where the variables are p_n^m for all $n \in \mathcal{T}$ and $m = 1 \dots M_n$. Clearly, for any link in m th multicast transmission of node n , i.e., $l \in \mathcal{O}^m(n)$, interference at $rec(l)$ is created by the other multicast transmissions of node n itself and by multicast transmissions of other nodes. The $\max(\cdot)$ operator in the denominator of SINR expressions is used to impose mutually exclusive multicast transmissions, e.g., if node 6 in Fig. 3 has singlepacket reception capability, then $\mathcal{O}^2(1)$ and $\mathcal{O}^1(2)$ are mutually exclusive.

III. ALGORITHM DERIVATION

For the sake of clarity, let us first address the case of singlecast networks. Extension to multicast case is presented separately in

⁴For the sake of clarity we consider only the case of sum power constraints for each transmitter node. However, supplementary sum power constraints can be also handled by the proposed algorithm. For example, in the case cellular downlink employing cooperation of several multiantenna base station, sum power constraints per subsets of nodes (one subset of nodes corresponds to a base station) should be also considered [40].

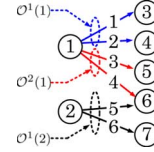


Fig. 3. Multicast network: Different colors represents different multicast transmissions. $\mathcal{T} = \{1, 2\}$, $M_1 = 2$, $M_2 = 1$, $\mathcal{O}^1(1) = \{1, 2\}$, $\mathcal{O}^2(1) = \{3, 4\}$, and $\mathcal{O}^1(2) = \{5, 6\}$.

Section V. We start by equivalently reformulating the original problem (2) as minimization of a nonconvex function over an L -dimensional rectangle. Then, we describe our proposed algorithm based on a branch and bound technique [49] to minimize the nonconvex function over the L -dimensional rectangle.

By introducing auxiliary variables γ_l , $l \in \mathcal{L}$ we first reformulate problem (2) in the following equivalent form:

$$\begin{aligned} & \text{minimize} && \sum_{l \in \mathcal{L}} -\beta_l \log(1 + \gamma_l) \\ & \text{subject to} && \gamma_l \leq \frac{g_l p_l}{\sigma^2 + \sum_{j \neq l} g_{jl} p_j}, \quad l \in \mathcal{L} \\ & && \sum_{l \in \mathcal{O}(n)} p_l \leq p_n^{\max}, \quad n \in \mathcal{T} \\ & && p_l \geq 0, \quad l \in \mathcal{L}, \end{aligned} \quad (4)$$

where the variables are $\{p_l, \gamma_l\}_{l \in \mathcal{L}}$. The equivalence between (2) and (4) follows from the monotone increasing property of the $\log(\cdot)$ function. Clearly, any feasible γ_l , $l \in \mathcal{L}$ in (4) represents an achievable SINR value for link l . Let us denote the objective function of (4) by $f_0(\boldsymbol{\gamma}) = \sum_{l \in \mathcal{L}} -\beta_l \log(1 + \gamma_l)$ and the feasible set for variables $\boldsymbol{\gamma} = [\gamma_1, \dots, \gamma_L]^T$ (or the achievable SINR values) by \mathcal{G} , i.e.,

$$\mathcal{G} = \left\{ \boldsymbol{\gamma} \left| \begin{array}{l} \gamma_l \leq \frac{g_l p_l}{\sigma^2 + \sum_{j \neq l} g_{jl} p_j}, \quad l \in \mathcal{L} \\ \sum_{l \in \mathcal{O}(n)} p_l \leq p_n^{\max}, \quad n \in \mathcal{T} \\ p_l \geq 0, \quad l \in \mathcal{L} \end{array} \right. \right\}. \quad (5)$$

The optimal value of (4) can be expressed compactly as $t^* = \inf_{\boldsymbol{\gamma} \in \mathcal{G}} f_0(\boldsymbol{\gamma})$.

For clarity, let us define a new function $\tilde{f} : \mathbb{R}_+^L \rightarrow \mathbb{R}$ as

$$\tilde{f}(\boldsymbol{\gamma}) = \begin{cases} f_0(\boldsymbol{\gamma}) & \boldsymbol{\gamma} \in \mathcal{G} \\ 0 & \text{otherwise} \end{cases} \quad (6)$$

$$\begin{aligned} & \text{maximize} && \sum_{n \in \mathcal{T}} \sum_{m=1}^{M_n} \beta_n^m \min_{l \in \mathcal{O}^m(n)} \log \left(1 + \frac{g_l p_n^m}{\sigma^2 + \sum_{j \in \mathcal{T}, j \neq n} \sum_{k=1}^{M_j} p_j^k \max_{i \in \mathcal{O}^k(j)} g_{il} + \sum_{k=1, k \neq m}^{M_n} p_n^k \max_{i \in \mathcal{O}^k(n)} g_{il}} \right) \\ & \text{subject to} && \sum_{m=1}^{M_n} p_n^m \leq p_n^{\max}, \quad n \in \mathcal{T} \\ & && p_n^m \geq 0, \quad n \in \mathcal{T}, m = 1 \dots M_n. \end{aligned} \quad (3)$$

and note that for any $\mathcal{S} \subseteq \mathbb{R}_+^L$ such that $\mathcal{G} \subseteq \mathcal{S}$, we have

$$\inf_{\gamma \in \mathcal{S}} \tilde{f}(\gamma) = \inf_{\gamma \in \mathcal{G}} f_0(\gamma) = t^*, \quad (7)$$

where the first equality follows from the fact that for any $\gamma \in \mathbb{R}_+^L$ we have $f_0(\gamma) \leq 0$. It is also worth noting that the function \tilde{f} is nonconvex over \mathcal{S} and f_0 is a global lower bound on \tilde{f} , i.e., $f_0(\gamma) \leq \tilde{f}(\gamma)$ for all $\gamma \in \mathcal{S}$.

Let us now define the L -dimensional rectangle $\mathcal{Q}_{\text{init}} = \left\{ \gamma \mid 0 \leq \gamma_l \leq \frac{\text{gUP}_{\text{tran}}^{\max}(l)}{\sigma^2}, l \in \mathcal{L} \right\}$ which encloses the set of all achievable SINR values, i.e., $\mathcal{G} \subseteq \mathcal{Q}_{\text{init}}$. By using (7), it follows that $t^* = \inf_{\gamma \in \mathcal{Q}_{\text{init}}} \tilde{f}(\gamma)$. Thus, we have reformulated

(2) equivalently as a minimization of the nonconvex function \tilde{f} over the rectangle $\mathcal{Q}_{\text{init}}$. In what follows we show how branch and bound technique is used to minimize \tilde{f} over $\mathcal{Q}_{\text{init}}$.

For any L -dimensional rectangle⁵ $\mathcal{Q} \subseteq \mathcal{Q}_{\text{init}}$, let us first define the following function:

$$\phi_{\min}(\mathcal{Q}) = \inf_{\gamma \in \mathcal{Q}} \tilde{f}(\gamma). \quad (8)$$

It can be easily observed that

$$\phi_{\min}(\mathcal{Q}_{\text{init}}) = \inf_{\gamma \in \mathcal{Q}_{\text{init}}} \tilde{f}(\gamma) = t^*. \quad (9)$$

The key idea of the branch and bound method is to generate a sequence of asymptotically tight upper and lower bounds for $\phi_{\min}(\mathcal{Q}_{\text{init}})$. At each iteration k , the lower bound L_k and the upper bound U_k are updated by partitioning $\mathcal{Q}_{\text{init}}$ into smaller rectangles. To ensure the convergence, the bounds should become tight as the number of rectangles in the partition of $\mathcal{Q}_{\text{init}}$ grows. To do this, the branch and bound method uses two functions $\phi_{\text{ub}}(\mathcal{Q})$ and $\phi_{\text{lb}}(\mathcal{Q})$, defined for any rectangle $\mathcal{Q} \subseteq \mathcal{Q}_{\text{init}}$ such that following conditions are satisfied [49].

C1) The functions $\phi_{\text{lb}}(\mathcal{Q})$ and $\phi_{\text{ub}}(\mathcal{Q})$ compute a lower bound and an upper bound respectively on $\phi_{\min}(\mathcal{Q})$, i.e.,

$$\forall \mathcal{Q} \subseteq \mathcal{Q}_{\text{init}} \text{ we have } \phi_{\text{lb}}(\mathcal{Q}) \leq \phi_{\min}(\mathcal{Q}) \leq \phi_{\text{ub}}(\mathcal{Q}). \quad (10)$$

C2) As the maximum half length of the sides of \mathcal{Q} (i.e., $\text{size}(\mathcal{Q}) = \frac{1}{2} \max_{l \in \mathcal{L}} \{\gamma_{l,\max} - \gamma_{l,\min}\}$) goes to zero, the difference between the upper and lower bounds uniformly converges to zero, i.e.

$$\forall \epsilon > 0 \exists \delta > 0 \text{ such that } \forall \mathcal{Q} \subseteq \mathcal{Q}_{\text{init}}, \text{size}(\mathcal{Q}) \leq \delta \Rightarrow \phi_{\text{ub}}(\mathcal{Q}) - \phi_{\text{lb}}(\mathcal{Q}) \leq \epsilon. \quad (11)$$

For the sake of clarity, the definition and computation of ϕ_{lb} and ϕ_{ub} is described in Section IV. In the remaining of this section we will present the proposed branch and bound method in more detail.

Let ϵ be an *a priori* specified tolerance. Algorithm starts by computing $\phi_{\text{ub}}(\mathcal{Q}_{\text{init}})$ and $\phi_{\text{lb}}(\mathcal{Q}_{\text{init}})$. If $\phi_{\text{ub}}(\mathcal{Q}_{\text{init}}) - \phi_{\text{lb}}(\mathcal{Q}_{\text{init}}) \leq \epsilon$, the algorithm terminates and C1 in (10) confirms that we have an upper bound $\phi_{\text{ub}}(\mathcal{Q}_{\text{init}})$ which is at most ϵ -away from the optimal value t^* . Otherwise, we start partitioning $\mathcal{Q}_{\text{init}}$ into smaller rectangles. At the k th

⁵A L -dimensional rectangle \mathcal{Q} is defined as $\mathcal{Q} = \{\gamma \mid \gamma_{l,\min} \leq \gamma_l \leq \gamma_{l,\max}, l \in \mathcal{L}\}$, where $\gamma_{l,\min}$ and $\gamma_{l,\max}$ are real numbers such that $\gamma_{l,\min} \leq \gamma_{l,\max}$ for all $l \in \mathcal{L}$.

partitioning step, $\mathcal{Q}_{\text{init}}$ is split into k rectangles such that $\mathcal{Q}_{\text{init}} = \mathcal{Q}_1 \cup \mathcal{Q}_2 \cup \dots \cup \mathcal{Q}_k$ and $\phi_{\text{ub}}(\mathcal{Q}_k)$ and $\phi_{\text{lb}}(\mathcal{Q}_k)$ are computed. Then the lower bound L_k and upper bound U_k are updated as follows:

$$\begin{aligned} L_k &= \min_{i \in \{1,2,\dots,k\}} \phi_{\text{lb}}(\mathcal{Q}_i) \leq \phi_{\min}(\mathcal{Q}_{\text{init}}) \\ &= t^* \leq \min_{i \in \{1,2,\dots,k\}} \phi_{\text{ub}}(\mathcal{Q}_i) = U_k. \end{aligned} \quad (12)$$

Note that the lower bound L_k and the upper bound U_k are refined at each step and they represent the best lower and upper bounds obtained so far. If the difference between new bounds become smaller than ϵ , then the algorithm terminates. Otherwise, further partitioning of $\mathcal{Q}_{\text{init}}$ is required until the difference between U_k and L_k is less than ϵ . The condition C2 in (11) ensures that, the difference $U_k - L_k$ eventually becomes smaller than ϵ for some finite k . The proposed algorithm based on branch and bound method can be summarized as follows.

Algorithm 1: Branch and Bound Methods for WSRMax

- 1) Initialization: given tolerance $\epsilon > 0$. Set $k = 1$, $\mathcal{B}_1 = \{\mathcal{Q}_{\text{init}}\}$, $U_1 = \phi_{\text{ub}}(\mathcal{Q}_{\text{init}})$ and $L_1 = \phi_{\text{lb}}(\mathcal{Q}_{\text{init}})$.
 - 2) Stopping criterion: if $U_k - L_k > \epsilon$ go to Step 3, otherwise STOP.
 - 3) Branching:
 - a) pick $\mathcal{Q} \in \mathcal{B}_k$ for which $\phi_{\text{lb}}(\mathcal{Q}) = L_k$ and set $\mathcal{Q}_k = \mathcal{Q}$.
 - b) split \mathcal{Q}_k along one of its longest edge into \mathcal{Q}_I and \mathcal{Q}_{II} .
 - c) form \mathcal{B}_{k+1} from \mathcal{B}_k by removing \mathcal{Q}_k and adding \mathcal{Q}_I and \mathcal{Q}_{II} .
 - 4) Bounding: compute $\phi_{\text{ub}}(\mathcal{Q}_I)$, $\phi_{\text{ub}}(\mathcal{Q}_{II})$, $\phi_{\text{lb}}(\mathcal{Q}_I)$, and $\phi_{\text{lb}}(\mathcal{Q}_{II})$.
 - a) set $U_{k+1} = \min\{U_k, \phi_{\text{ub}}(\mathcal{Q}_I), \phi_{\text{ub}}(\mathcal{Q}_{II})\}$.
 - b) set $L_{k+1} = \min\{L_k, \phi_{\text{lb}}(\mathcal{Q}_I), \phi_{\text{lb}}(\mathcal{Q}_{II})\}$.
 - 5) Pruning:
 - a) pick all $\mathcal{Q} \in \mathcal{B}_{k+1}$ for which $\phi_{\text{lb}}(\mathcal{Q}) \geq U_{k+1}$.
 - b) update \mathcal{B}_{k+1} by removing all \mathcal{Q} obtained in the above step (5-a).
 - 6) Set $k = k + 1$ and go to step (2).
-

The first step initializes the algorithm and the upper and lower bounds are computed over the initial rectangle $\mathcal{Q}_{\text{init}}$. The second step checks the difference between the best upper and lower bounds found so far (i.e., U_k and L_k given by (12)). The algorithm repeats steps 3 to 6 until $U_k - L_k < \epsilon$.

Step 3 is the *branching* mechanism of the algorithm. Here we adopt the following branching rule: select from the current partition of $\mathcal{Q}_{\text{init}}$ (i.e., \mathcal{B}_k) the rectangle with the smallest lower bound and split it in two smaller rectangles along its longest edge. Splitting the chosen rectangle along its longest edge ensures the convergence of the algorithm [49]. At step 4 the best upper bound U_k and the best lower bound L_k are updated according to (12).

Step 5 is used to eliminate (or prune) rectangles for which the lower bound is larger than the best upper bound found so far, since those rectangles can never contain a minimizer of the function \tilde{f} . Note that *pruning* does not affect the speed of the

main algorithm since none of the rectangles that were pruned will be selected later in the branching step 3 for further splitting. The advantage of pruning is the release of the memory used for storing unnecessary rectangles.

The convergence of the above algorithm is established by the following theorem.

Theorem 1: If for any $\mathcal{Q} \subseteq \mathcal{Q}_{\text{init}}$ with $\mathcal{Q} = \{\gamma \mid \gamma_{l,\min} \leq \gamma_l \leq \gamma_{l,\max}, l \in \mathcal{L}\}$, the functions $\phi_{\text{ub}}(\mathcal{Q})$ and $\phi_{\text{lb}}(\mathcal{Q})$ satisfy the conditions C1 and C2, then *Algorithm 1* converges in a finite number of iterations to a value arbitrarily close to t^* , i.e., $\forall \epsilon > 0, \exists K > 0$ such that $U_K - t^* \leq \epsilon$.

Proof: The proof is similar to the one provided in [65] and it is not reproduced here for the sake of brevity. ■

Note that the main challenge in designing a global optimization algorithm based on branch and bound method is to find cheaply computable functions $\phi_{\text{ub}}(\mathcal{Q})$ and $\phi_{\text{lb}}(\mathcal{Q})$ such that the conditions given in (10) and (11) are satisfied. Basically, the essence of the branch and bound method is based on the fact that for any $\mathcal{Q} \subseteq \mathcal{Q}_{\text{init}}$, the bounds $\phi_{\text{ub}}(\mathcal{Q})$ and $\phi_{\text{lb}}(\mathcal{Q})$ are substantially easier to compute than the true minimum $\phi_{\text{min}}(\mathcal{Q})$ [49].

IV. COMPUTATION OF UPPER BOUND AND LOWER BOUND

In this section we propose several candidates for $\phi_{\text{lb}}(\mathcal{Q})$ and $\phi_{\text{ub}}(\mathcal{Q})$ in Algorithm 1. First, we describe two basic lower and upper bound functions, prove that they satisfy the conditions C1 and C2 [see (10) and (11)], and present efficient methods for computing them. Computationally efficient better bounds are presented later in this section.

A. Basic Lower and Upper Bounds

Recall that $\mathcal{Q} = \{\gamma \mid \gamma_{l,\min} \leq \gamma_l \leq \gamma_{l,\max}, l \in \mathcal{L}\}$. We now define the functions $\phi_{\text{lb}}^{\text{Basic}}(\mathcal{Q})$ and $\phi_{\text{ub}}^{\text{Basic}}(\mathcal{Q})$ as

$$\phi_{\text{lb}}^{\text{Basic}}(\mathcal{Q}) = \begin{cases} f_0(\gamma_{\max}) & \gamma_{\min} \in \mathcal{G} \\ 0 & \text{otherwise,} \end{cases} \quad (13)$$

$$\phi_{\text{ub}}^{\text{Basic}}(\mathcal{Q}) = \tilde{f}(\gamma_{\min}) = \begin{cases} f_0(\gamma_{\min}) & \gamma_{\min} \in \mathcal{G} \\ 0 & \text{otherwise,} \end{cases} \quad (14)$$

where $\gamma_{\max} = [\gamma_{1,\max}, \dots, \gamma_{L,\max}]^T$, $\gamma_{\min} = [\gamma_{1,\min}, \dots, \gamma_{L,\min}]^T$ and \mathcal{G} is defined in (5). Note that the most computationally expensive part of evaluating $\phi_{\text{lb}}^{\text{Basic}}(\mathcal{Q})$ and $\phi_{\text{ub}}^{\text{Basic}}(\mathcal{Q})$ is to check the condition $\gamma_{\min} \in \mathcal{G}$. An efficient method for checking this condition is provided soon after the following important properties of functions $\phi_{\text{lb}}^{\text{Basic}}$ and $\phi_{\text{ub}}^{\text{Basic}}$ are established.

Lemma 1: The functions $\phi_{\text{lb}}^{\text{Basic}}(\mathcal{Q})$ and $\phi_{\text{ub}}^{\text{Basic}}(\mathcal{Q})$ satisfy the condition C1.

Proof: In the case of $\gamma_{\min} \notin \mathcal{G}$ we can easily see that $\phi_{\text{lb}}^{\text{Basic}}(\mathcal{Q}) = \phi_{\text{min}}(\mathcal{Q}) = \phi_{\text{ub}}^{\text{Basic}}(\mathcal{Q}) = 0$ and therefore the inequalities in C1 holds with equalities. In the case of $\gamma_{\min} \in \mathcal{G}$ we notice that

$$\phi_{\text{min}}(\mathcal{Q}) = \inf_{\gamma \in \mathcal{Q}} \tilde{f}(\gamma) \leq \tilde{f}(\gamma_{\min}) = f_0(\gamma_{\min}) = \phi_{\text{ub}}^{\text{Basic}}(\mathcal{Q}). \quad (15)$$

The first equality follows from (8), the inequality follows since $\gamma_{\min} \in \mathcal{Q}$ and the second equality follows from (6). Moreover, we have

$$\phi_{\text{min}}(\mathcal{Q}) = \inf_{\gamma \in \mathcal{Q}} \tilde{f}(\gamma) \geq \inf_{\gamma \in \mathcal{Q}} f_0(\gamma) = f_0(\gamma_{\max}) = \phi_{\text{lb}}^{\text{Basic}}(\mathcal{Q}), \quad (16)$$

where the inequality follows from the fact that $\tilde{f}(\gamma) \geq f_0(\gamma)$ and the second equality is from the fact that \mathcal{Q} is a rectangle and $f_0(\gamma)$ is monotonically decreasing in each variable γ_l , $l \in \mathcal{L}$. From (15) and (16), we conclude that $\phi_{\text{lb}}^{\text{Basic}}(\mathcal{Q}) \leq \phi_{\text{min}}(\mathcal{Q}) \leq \phi_{\text{ub}}^{\text{Basic}}(\mathcal{Q})$. ■

Lemma 2: The functions $\phi_{\text{lb}}^{\text{Basic}}(\mathcal{Q})$ and $\phi_{\text{ub}}^{\text{Basic}}(\mathcal{Q})$ satisfy the condition C2.

Proof: We first show that the function $f_0(\gamma) = \sum_{l \in \mathcal{L}} -\beta_l \log(1 + \gamma_l)$ is Lipschitz continuous on \mathbb{R}_+^L with the constant $D = \sqrt{\sum_{l \in \mathcal{L}} \beta_l^2}$, i.e.,

$$|f_0(\mu) - f_0(\nu)| \leq D \|\mu - \nu\|_2 \quad (17)$$

for all $\mu, \nu \in \mathbb{R}_+^L$. We start by noting that $f_0(\gamma)$ is convex. Therefore, for all $\mu, \nu \in \mathbb{R}_+^L$ we have [66, Sec. 3.1.3]

$$f_0(\mu) - f_0(\nu) \leq \nabla f_0(\mu)(\mu - \nu). \quad (18)$$

Without loss of generality, we can assume that $f_0(\mu) - f_0(\nu) \geq 0$ and thus⁶,

$$|f_0(\mu) - f_0(\nu)| \leq |\nabla f_0(\mu)^T(\mu - \nu)| \quad (19)$$

$$\leq \|\nabla f_0(\mu)\|_2 \|\mu - \nu\|_2 \quad (20)$$

$$\leq \max_{\gamma \in \mathbb{R}_+^L} \|\nabla f_0(\gamma)\|_2 \|\mu - \nu\|_2 \quad (21)$$

$$= \max_{\gamma \in \mathbb{R}_+^L} \sqrt{\sum_{l \in \mathcal{L}} \frac{\beta_l^2}{(1 + \gamma_l)^2}} \|\mu - \nu\|_2 \quad (22)$$

$$= D \|\mu - \nu\|_2, \quad (23)$$

where (19) follows from (18), (20) follows from the Cauchy-Schwarz inequality, (21) follows from the maximization operation, (22) follows by noting that $[\nabla f_0(\gamma)]_l = \frac{\beta_l}{(1 + \gamma_l)}$, $l \in \mathcal{L}$, and (23) follows by setting $\gamma_l = 0$ for all $l \in \mathcal{L}$.

Now we can write the following relations:

$$\phi_{\text{ub}}^{\text{Basic}}(\mathcal{Q}) - \phi_{\text{lb}}^{\text{Basic}}(\mathcal{Q}) \leq f_0(\gamma_{\min}) - f_0(\gamma_{\max}) \quad (24)$$

$$\leq D \|\gamma_{\min} - \gamma_{\max}\|_2 \quad (25)$$

$$= D \left\| \sum_{l \in \mathcal{L}} (\gamma_{l,\max} - \gamma_{l,\min}) \mathbf{e}_l \right\|_2 \quad (26)$$

$$\leq D \sum_{l \in \mathcal{L}} (\gamma_{l,\max} - \gamma_{l,\min}) \quad (27)$$

$$\leq 2DL \text{size}(\mathcal{Q}). \quad (28)$$

The first inequality (24) follows from (13) and (14) by noting that f_0 is nonincreasing, (25) follows from (17), (26), follows clearly by noting that \mathbf{e}_l is l th standard unit vector, (27) follows from triangle inequality, and (28) follows from the definition of size(\mathcal{Q}) (see C2). Thus, for any given $\epsilon > 0$, we can select δ such that $\delta \leq \frac{\epsilon}{2DL}$ which in turns implies that condition C2 is satisfied. ■

In the sequel, we present a computationally efficient method to check the condition $\gamma_{\min} \in \mathcal{G}$ which is central in computing $\phi_{\text{lb}}^{\text{Basic}}(\mathcal{Q})$ and $\phi_{\text{ub}}^{\text{Basic}}(\mathcal{Q})$ efficiently. Without loss of generality, we can assume that $\gamma_{\min} \succ \mathbf{0}$. Note that the method can be

⁶Otherwise, we can obtain exactly the same results by interchanging μ and ν in (18), i.e., $f_0(\nu) - f_0(\mu) \leq \nabla f_0(\nu)(\nu - \mu)$.

extended to the case where there are links l for which $\gamma_{l,\min} = 0$ in a straightforward manner.⁷

Let us first consider the first set of inequalities in the description of \mathcal{G} , i.e.,

$$\gamma_l \leq \frac{g_{ll} p_l}{\sigma^2 + \sum_{j \neq l} g_{jl} p_j}, \quad l \in \mathcal{L}. \quad (29)$$

Let $\boldsymbol{\gamma} = [\gamma_1, \dots, \gamma_L]^T$ and $\mathbf{p} = [p_1, \dots, p_L]^T$. By rearranging the terms, (29) can be equivalently expressed as [37], [67]

$$(\mathbf{I} - \mathbf{B}(\boldsymbol{\gamma})\mathbf{G})\mathbf{p} \succeq \sigma^2 \mathbf{B}(\boldsymbol{\gamma})\mathbf{1}, \quad (30)$$

where the matrices $\mathbf{B}(\boldsymbol{\gamma}) \in \mathbb{R}_+^{L \times L}$ and $\mathbf{G} \in \mathbb{R}_+^{L \times L}$ are defined by

$$\mathbf{B}(\boldsymbol{\gamma}) = \text{diag} \left\{ \frac{\gamma_1}{g_{11}}, \dots, \frac{\gamma_L}{g_{LL}} \right\};$$

$$[\mathbf{G}]_{i,j} = \begin{cases} g_{ji} & i \neq j \\ 0 & \text{otherwise.} \end{cases} \quad (31)$$

For the notational simplicity, let

$$\mathbf{A}(\boldsymbol{\gamma}) = \mathbf{I} - \mathbf{B}(\boldsymbol{\gamma})\mathbf{G} \text{ and } \mathbf{b}(\boldsymbol{\gamma}) = \sigma^2 \mathbf{B}(\boldsymbol{\gamma})\mathbf{1}. \quad (32)$$

Thus, (29) can be compactly expressed as $\mathbf{A}(\boldsymbol{\gamma})\mathbf{p} \succeq \mathbf{b}(\boldsymbol{\gamma})$. Let us denote the spectral radius [68, p. 5] of matrix $\mathbf{B}(\boldsymbol{\gamma})\mathbf{G}$ by $\rho(\mathbf{B}(\boldsymbol{\gamma})\mathbf{G})$. The following theorem helps us to check if $\boldsymbol{\gamma} \in \mathcal{G}$.

Theorem 2: For any $\boldsymbol{\gamma} \succ \mathbf{0}$, the following implications hold:

- 1) $\rho(\mathbf{B}(\boldsymbol{\gamma})\mathbf{G}) \geq 1 \implies \boldsymbol{\gamma} \notin \mathcal{G}$.
- 2) $\rho(\mathbf{B}(\boldsymbol{\gamma})\mathbf{G}) < 1$ and $\sum_{l \in \mathcal{O}(n)} p_l \leq p_n^{\max}$ for all $n \in \mathcal{T}$, where $\mathbf{p} = \mathbf{A}^{-1}(\boldsymbol{\gamma})\mathbf{b}(\boldsymbol{\gamma}) \implies \boldsymbol{\gamma} \in \mathcal{G}$.
- 3) $\rho(\mathbf{B}(\boldsymbol{\gamma})\mathbf{G}) < 1$ and $\exists n \in \mathcal{T}$ such that $\sum_{l \in \mathcal{O}(n)} p_l > p_n^{\max}$, where $\mathbf{p} = \mathbf{A}^{-1}(\boldsymbol{\gamma})\mathbf{b}(\boldsymbol{\gamma}) \implies \boldsymbol{\gamma} \notin \mathcal{G}$.

Proof: See Appendix A. \blacksquare

Based on Theorem 2 the condition $\boldsymbol{\gamma}_{\min} \in \mathcal{G}$ can be checked as follows:

Algorithm 2: Checking for Condition $\boldsymbol{\gamma}_{\min} \in \mathcal{G}$

- 1) Construct $\mathbf{B}(\boldsymbol{\gamma}_{\min})$ and \mathbf{G} according to (31).
 - 2) If $\rho(\mathbf{B}(\boldsymbol{\gamma}_{\min})\mathbf{G}) \geq 1$, then $\boldsymbol{\gamma}_{\min} \notin \mathcal{G}$ and STOP. Otherwise, let $\mathbf{p} = \mathbf{A}^{-1}(\boldsymbol{\gamma}_{\min})\mathbf{b}(\boldsymbol{\gamma}_{\min})$.
 - 3) If $\sum_{l \in \mathcal{O}(n)} p_l \leq p_n^{\max}$ for all $n \in \mathcal{T}$, then $\boldsymbol{\gamma}_{\min} \in \mathcal{G}$ and STOP. Otherwise, $\boldsymbol{\gamma}_{\min} \notin \mathcal{G}$ and STOP.
-

B. Improved Lower and Upper Bounds

Finding tighter bounds is very important as they can increase substantially the convergence speed of Algorithm 1. By exploiting the monotonically nonincreasing property of f_0 ,⁸ one improved lower bound and two improved upper bounds are proposed in this subsection. Efficient methods to compute them are provided as well.

Note that, in the case of $\boldsymbol{\gamma}_{\min} \notin \mathcal{G}$ [i.e., $\mathcal{Q} \cap \mathcal{G} = \emptyset$, see Fig. 4(a)], $f(\boldsymbol{\gamma}) = 0$ for any $\boldsymbol{\gamma} \in \mathcal{Q}$. Thus, both the basic lower bound (13) and the basic upper bound (14) are trivially zero and

⁷In this case, checking the original condition $\boldsymbol{\gamma}_{\min} \in \mathcal{G}$ is equivalent to checking a modified condition $\tilde{\boldsymbol{\gamma}}_{\min} \in \tilde{\mathcal{G}}$ where $\tilde{\boldsymbol{\gamma}}_{\min}$ and $\tilde{\mathcal{G}}$ are obtained by eliminating the dimensions (or link indexes) for which $\gamma_{l,\min} = 0$ and thus, we have $\tilde{\boldsymbol{\gamma}}_{\min} \succ \mathbf{0}$.

⁸That is, $\gamma_1 \leq \gamma_2 \implies f_0(\gamma_1) \geq f_0(\gamma_2)$

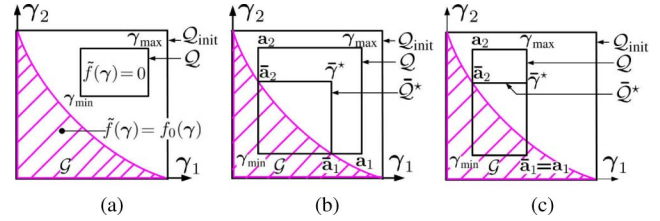


Fig. 4. Illustration of the sets \mathcal{G} , $\mathcal{Q}_{\text{init}}$, \mathcal{Q} , and $\tilde{\mathcal{Q}}^*$ in a 2-dimensional space.

no further improvement is possible since they are tight. Consequently, tighter bounds can be found only in the case $\boldsymbol{\gamma}_{\min} \in \mathcal{G}$ [i.e., $\mathcal{Q} \cap \mathcal{G} \neq \emptyset$, see Fig. 4(b)]. Thus, we consider only this case in the sequel, unless otherwise specified.

1) *Improved Lower Bound:* Roughly speaking, a tighter lower bound can be obtained as follows. We first construct the smallest rectangle $\tilde{\mathcal{Q}}^* \subseteq \mathcal{Q}$ which encloses the intersection $\mathcal{Q} \cap \mathcal{G}$ [see Fig. 4(b)]. Let us denote this rectangle as $\tilde{\mathcal{Q}}^* = \{\boldsymbol{\gamma} | \gamma_{l,\min} \leq \gamma_l \leq \tilde{\gamma}_l^*, l \in \mathcal{L}\}$. The improved lower bound is given by $f_0(\tilde{\gamma}_1^*, \dots, \tilde{\gamma}_L^*)$.⁹

Recall that $\mathcal{Q} = \{\boldsymbol{\gamma} | \gamma_{l,\min} \leq \gamma_l \leq \gamma_{l,\max}, l \in \mathcal{L}\}$. For any $\mathcal{Q} \subseteq \mathcal{Q}_{\text{init}}$, the improved lower bound can be formally expressed as

$$\phi_{\text{lb}}^{\text{Imp}}(\mathcal{Q}) = \begin{cases} f_0(\tilde{\boldsymbol{\gamma}}^*) & \boldsymbol{\gamma}_{\min} \in \mathcal{G} \\ 0 & \text{otherwise,} \end{cases} \quad (33)$$

where $\tilde{\boldsymbol{\gamma}}^* = [\tilde{\gamma}_1^*, \dots, \tilde{\gamma}_L^*]^T$ and $\tilde{\gamma}_i^*$ is the optimal value of the following optimization problem:

$$\begin{aligned} & \text{maximize} && \frac{g_{ii} p_i}{\sigma^2 + \sum_{j \neq i} g_{ji} p_j} \\ & \text{subject to} && \frac{g_{ii} p_i}{\sigma^2 + \sum_{j \neq i} g_{ji} p_j} \leq \gamma_{i,\max} \\ & && \gamma_{l,\min} = \frac{g_{ll} p_l}{\sigma^2 + \sum_{j \neq l} g_{jl} p_j}, \quad l \in \mathcal{L} \setminus \{i\} \\ & && \sum_{l \in \mathcal{O}(n)} p_l \leq p_n^{\max}, \quad n \in \mathcal{T} \\ & && p_l \geq 0, \quad l \in \mathcal{L}, \end{aligned} \quad (34)$$

where the optimization variables are $\{p_l\}_{l \in \mathcal{L}}$. The first inequality constraint ensures that $\tilde{\mathcal{Q}}^* \subseteq \mathcal{Q}$ and it is active if and only if the corner point $\mathbf{a}_i = \boldsymbol{\gamma}_{\min} + (\gamma_{i,\max} - \gamma_{i,\min})\mathbf{e}_i$ lies inside \mathcal{G} , i.e., $\mathbf{a}_i \in \mathcal{G}$ [see \mathbf{a}_1 in Fig. 4(c)]. Therefore, when $\mathbf{a}_i \in \mathcal{G}$, $\tilde{\gamma}_i^* = \gamma_{i,\max}$. Otherwise (i.e., $\mathbf{a}_i \notin \mathcal{G}$), $\tilde{\gamma}_i^*$ is limited by the power constraints. In this case, the first constraint of (34) can be safely dropped and the resulting problem can be readily converted into a standard geometric program (GP) [66] so that the solution can be obtained numerically by using a GP solver, e.g., GGPLAB, GPPOSY, GPCVX [69]. However, it turns out that, the particular structure of (34) allows us to find analytically the optimal value. This provides a more computationally efficient way to compute $\phi_{\text{lb}}^{\text{Imp}}(\mathcal{Q})$ without relying on

⁹Further improvement can be obtained by constructing an outer polyblock approximation [50] for $\tilde{\mathcal{Q}}^* \cap \mathcal{G}$ that lies inside $\tilde{\mathcal{Q}}^*$. If $\{\mathbf{v}_i\}_{i \in \mathcal{V}}$ are the proper vertices of the polyblock, it is easy to see that an improved bound is given by $\min_{i \in \mathcal{V}} f_0(\mathbf{v}_i)$. Though interesting, in this paper we do not consider these possible extensions due to the space limitation, but we refer the reader to [48, Ch. 2, Sec. 7] where similar bound improving techniques are discussed in the context of (difference of) monotonic optimization problems.

a GP solver. This method is described soon after the following important property of $\phi_{\text{lb}}^{\text{Imp}}(\mathcal{Q})$ is established.

Lemma 3: For any $\mathcal{Q} \subseteq \mathcal{Q}_{\text{init}}$ the lower bound $\phi_{\text{lb}}^{\text{Imp}}(\mathcal{Q})$ (33) is better than the basic lower bound $\phi_{\text{lb}}^{\text{Basic}}(\mathcal{Q})$ (13), i.e., $\phi_{\text{min}}(\mathcal{Q}) \geq \phi_{\text{lb}}^{\text{Imp}}(\mathcal{Q}) \geq \phi_{\text{lb}}^{\text{Basic}}(\mathcal{Q})$.

Proof: If $\boldsymbol{\gamma}_{\text{min}} \notin \mathcal{G}$, we have $\phi_{\text{min}}(\mathcal{Q}) = \phi_{\text{lb}}^{\text{Imp}}(\mathcal{Q}) = \phi_{\text{lb}}^{\text{Basic}}(\mathcal{Q}) = 0$. Otherwise, i.e., when $\boldsymbol{\gamma}_{\text{min}} \in \mathcal{G}$ we obtain (35), shown at the bottom of the page, where the first equality is from (8), the second equality follows from the fact that $\mathcal{G} \cap \mathcal{Q}$ is nonempty and $\tilde{f}(\boldsymbol{\gamma}) = 0$ for all $\boldsymbol{\gamma} \in \mathcal{Q} \setminus (\mathcal{G} \cap \mathcal{Q})$, the third equality follows from $\tilde{f}(\boldsymbol{\gamma}) = f_0(\boldsymbol{\gamma})$ for all $\boldsymbol{\gamma} \in \mathcal{G} \cap \mathcal{Q}$, the first inequality follows by noting that $\tilde{\boldsymbol{\gamma}}^* \succeq \boldsymbol{\gamma}$ for all $\boldsymbol{\gamma} \in \mathcal{Q} \cap \mathcal{G}$ and f_0 is monotonically decreasing in each dimension, and the last inequality follows since $\boldsymbol{\gamma}_{\text{max}} \succeq \tilde{\boldsymbol{\gamma}}^*$ and f_0 is monotonically decreasing. ■

We describe now an efficient method to find $\tilde{\boldsymbol{\gamma}}_i^*$ by solving (34) when $\boldsymbol{\gamma}_{\text{min}} \in \mathcal{G}$ and $\mathbf{a}_i \notin \mathcal{G}$. We can assume without loss of generality that $\gamma_{l,\text{min}} > 0$ for all $l \in \mathcal{L} \setminus \{i\}$.¹⁰ The proposed method can be summarized as follows: by using the equality constraints we eliminate the $L-1$ variables $\{p_l\}_{l \in \mathcal{L} \setminus \{i\}}$ and transform problem (34) into a single variable optimization problem (with variable p_i). This facilitates finding the optimal power p_i^* (and implicitly $\tilde{\boldsymbol{\gamma}}_i^*$), in an efficient and straightforward manner.

For a detailed description of the above method it is useful to introduce a virtual network which is obtained from the original network by removing the i th link. Such a network is referred to as *reduced* network. For notational convenience let us define the following vectors and matrices associated to the reduced network: $\bar{\mathbf{p}}_i$ and $\tilde{\boldsymbol{\gamma}}_{\text{min},i}$ are obtained from \mathbf{p} and $\boldsymbol{\gamma}_{\text{min}}$ by removing the i th entries, i.e., $\bar{\mathbf{p}}_i = [p_1, \dots, p_{i-1}, p_{i+1}, \dots, p_L]^T$ and $\tilde{\boldsymbol{\gamma}}_{\text{min},i} = [\gamma_{1,\text{min}}, \dots, \gamma_{i-1,\text{min}}, \gamma_{i+1,\text{min}}, \dots, \gamma_{L,\text{min}}]^T$; similarly, $\bar{\mathbf{B}}_i(\tilde{\boldsymbol{\gamma}}_{\text{min},i})$ and $\bar{\mathbf{G}}_i$ are obtained from $\mathbf{B}(\boldsymbol{\gamma}_{\text{min}})$ and \mathbf{G} [see (31)] by removing the i th rows and the i th columns. It is important to note that if SINR vector $\boldsymbol{\gamma}_{\text{min}}$ is achievable in the original network then $\tilde{\boldsymbol{\gamma}}_{\text{min},i}$ is also achievable in the reduced network.

Now we turn to (34). By rearranging the terms, the equality constraints can be expressed compactly as

$$[\mathbf{I} - \bar{\mathbf{B}}_i(\tilde{\boldsymbol{\gamma}}_{\text{min},i})\bar{\mathbf{G}}_i]\bar{\mathbf{p}}_i + \mathbf{d}_i(\tilde{\boldsymbol{\gamma}}_{\text{min},i})p_i = \sigma^2\bar{\mathbf{B}}_i(\tilde{\boldsymbol{\gamma}}_{\text{min},i})\mathbf{1}, \quad (36)$$

where

¹⁰The proposed method can be extended to the case where there are links for which $\gamma_{l,\text{min}} = 0$ for some $l \in \mathcal{L} \setminus \{i\}$; In this case, the original problem (34) is equivalent to a modified problem obtained by eliminating the dimensions $l \in \mathcal{L} \setminus \{i\}$ (i.e., link indexes) for which $\gamma_{l,\text{min}} = 0$.

$$\mathbf{d}_i(\tilde{\boldsymbol{\gamma}}_{\text{min},i}) = - \left[\frac{g_{i1}\gamma_{1,\text{min}}}{g_{11}}, \dots, \frac{g_{i,i-1}\gamma_{i-1,\text{min}}}{g_{i-1,i-1}}, \right. \\ \left. \frac{g_{i,i+1}\gamma_{i+1,\text{min}}}{g_{i+1,i+1}}, \dots, \frac{g_{iL}\gamma_{L,\text{min}}}{g_{LL}} \right]^T.$$

Similarly to (32), let us denote

$$\bar{\mathbf{A}}_i(\tilde{\boldsymbol{\gamma}}_{\text{min},i}) = \mathbf{I} - \bar{\mathbf{B}}_i(\tilde{\boldsymbol{\gamma}}_{\text{min},i})\bar{\mathbf{G}}_i; \quad \bar{\mathbf{b}}_i(\tilde{\boldsymbol{\gamma}}_{\text{min},i}) = \sigma^2\bar{\mathbf{B}}_i(\tilde{\boldsymbol{\gamma}}_{\text{min},i})\mathbf{1}, \quad (37)$$

and rewrite (36) equivalently as

$$\bar{\mathbf{A}}_i(\tilde{\boldsymbol{\gamma}}_{\text{min},i})\bar{\mathbf{p}}_i + \mathbf{d}_i(\tilde{\boldsymbol{\gamma}}_{\text{min},i})p_i = \bar{\mathbf{b}}_i(\tilde{\boldsymbol{\gamma}}_{\text{min},i}). \quad (38)$$

Since $\boldsymbol{\gamma}_{\text{min}} \in \mathcal{G}$ it follows that the SINR vector $\tilde{\boldsymbol{\gamma}}_{\text{min},i} \succ \mathbf{0}$ is achievable in the reduced network. Thus, Theorem 2 (applied to the reduced network) implies that the spectral radius of the matrix $\bar{\mathbf{B}}_i(\tilde{\boldsymbol{\gamma}}_{\text{min},i})\bar{\mathbf{G}}_i$ is strictly smaller than one, i.e., $\rho(\bar{\mathbf{B}}_i(\tilde{\boldsymbol{\gamma}}_{\text{min},i})\bar{\mathbf{G}}_i) < 1$. This, in turn, ensures that matrix $\bar{\mathbf{A}}_i(\tilde{\boldsymbol{\gamma}}_{\text{min},i})$ is invertible and its inverse has nonnegative entries, i.e., $\bar{\mathbf{A}}_i^{-1}(\tilde{\boldsymbol{\gamma}}_{\text{min},i}) \succeq \mathbf{0}$ [68, Th. 2.5.3, items 2 and 17]. Therefore, we can parameterize all solutions of (36), using p_i as a free parameter [66, Sect. C.5, p. 681]. Thus, we obtain (39), shown at the bottom of the page, where $q_i = 1$, $s_i = 0$, $\bar{\mathbf{q}}_i = -\bar{\mathbf{A}}_i^{-1}(\tilde{\boldsymbol{\gamma}}_{\text{min},i})\mathbf{d}_i(\tilde{\boldsymbol{\gamma}}_{\text{min},i})$ and $\bar{\mathbf{s}}_i = \bar{\mathbf{A}}_i^{-1}(\tilde{\boldsymbol{\gamma}}_{\text{min},i})\bar{\mathbf{b}}_i(\tilde{\boldsymbol{\gamma}}_{\text{min},i})$. The vectors $\bar{\mathbf{q}}_i$ and $\bar{\mathbf{s}}_i$ are introduced for notational simplicity and they have the following structure: $\bar{\mathbf{q}}_i = [q_1, \dots, q_{i-1}, q_{i+1}, \dots, q_L]^T$ and $\bar{\mathbf{s}}_i = [s_1, \dots, s_{i-1}, s_{i+1}, \dots, s_L]^T$. Furthermore, since $\bar{\mathbf{A}}_i^{-1}(\tilde{\boldsymbol{\gamma}}_{\text{min},i}) \succeq \mathbf{0}$ and by noting that $\mathbf{d}_i(\tilde{\boldsymbol{\gamma}}_{\text{min},i}) \preceq \mathbf{0}$ and $\bar{\mathbf{b}}_i(\tilde{\boldsymbol{\gamma}}_{\text{min},i}) \succeq \mathbf{0}$ [see (37)], we can see that all entries in vectors $\bar{\mathbf{q}}_i$ and $\bar{\mathbf{s}}_i$ are nonnegative, i.e., $\bar{\mathbf{q}}_i \succeq \mathbf{0}$ and $\bar{\mathbf{s}}_i \succeq \mathbf{0}$. Finally, we can rewrite parametrization (39) as

$$p_j = q_j p_i + s_j, \quad j \in \mathcal{L}, \quad (40)$$

where $q_j \geq 0$, $s_j \geq 0$ for all $j \in \mathcal{L}$, and $q_i = 1$, $s_i = 0$.

Next we use the parametrization (40) to convert (34) (with L power variables) into an equivalent one with a single power variable p_i . To do this, we first express the objective function of (34) $g_i(\mathbf{p})$ as a function of single variable p_i , i.e.,

$$g_i(\mathbf{p}) = \frac{g_{ii}p_i}{\sigma^2 + \sum_{j \neq i} g_{ji}p_j} \\ = \frac{g_{ii}p_i}{\sigma^2 + \sum_{j \neq i} g_{ji}(q_j p_i + s_j)} = \bar{g}_i(p_i). \quad (41)$$

$$\phi_{\text{min}}(\mathcal{Q}) = \inf_{\boldsymbol{\gamma} \in \mathcal{Q}} \tilde{f}(\boldsymbol{\gamma}) = \inf_{\boldsymbol{\gamma} \in \mathcal{G} \cap \mathcal{Q}} \tilde{f}(\boldsymbol{\gamma}) = \inf_{\boldsymbol{\gamma} \in \mathcal{G} \cap \mathcal{Q}} f_0(\boldsymbol{\gamma}) \geq f_0(\tilde{\boldsymbol{\gamma}}^*) = \phi_{\text{lb}}^{\text{Imp}}(\mathcal{Q}) \geq f_0(\boldsymbol{\gamma}_{\text{max}}) = \phi_{\text{lb}}^{\text{Basic}}(\mathcal{Q}). \quad (35)$$

$$\begin{bmatrix} \bar{\mathbf{p}}_i \\ p_i \end{bmatrix} = \begin{bmatrix} -\bar{\mathbf{A}}_i^{-1}(\tilde{\boldsymbol{\gamma}}_{\text{min},i})\mathbf{d}_i(\tilde{\boldsymbol{\gamma}}_{\text{min},i}) \\ 1 \end{bmatrix} p_i + \begin{bmatrix} \bar{\mathbf{A}}_i^{-1}(\tilde{\boldsymbol{\gamma}}_{\text{min},i})\bar{\mathbf{b}}_i(\tilde{\boldsymbol{\gamma}}_{\text{min},i}) \\ 0 \end{bmatrix} = \begin{bmatrix} \bar{\mathbf{q}}_i \\ q_i \end{bmatrix} p_i + \begin{bmatrix} \bar{\mathbf{s}}_i \\ s_i \end{bmatrix} \quad (39)$$

The sum power constraints of (34) (i.e., $\sum_{l \in \mathcal{O}(n)} p_l \leq p_n^{\max}$, $n \in \mathcal{T}$) can be expressed as

$$p_i \leq \frac{p_n^{\max} - \sum_{l \in \mathcal{O}(n)} s_l}{\sum_{l \in \mathcal{O}(n)} q_l}, \quad n \in \mathcal{T}. \quad (42)$$

Furthermore, since $q_j \geq 0$, $s_j \geq 0$, all L nonnegativity power constraints of (34) can be replaced by $p_i \geq 0$, i.e., $p_i \geq 0$ in parametrization (40) implies that $p_j \geq 0$ for all $j \in \mathcal{L}$. Thus, (34) can be expressed equivalently as¹¹

$$\begin{aligned} & \text{maximize} && \bar{g}_i(p_i) \\ & \text{subject to} && p_i \leq \frac{p_n^{\max} - \sum_{l \in \mathcal{O}(n)} s_l}{\sum_{l \in \mathcal{O}(n)} q_l}, \quad n \in \mathcal{T} \\ & && p_i \geq 0, \end{aligned} \quad (43)$$

where the variable is p_i . By recalling that $s_l \geq 0$ for all $l \in \mathcal{L}$, it is easy to see that the first derivative of the objective function $\bar{g}_i(p_i)$ is strictly positive. Hence, the maximum $\bar{g}_i(p_i)$ can be found by increasing p_i until one power constraint become active. Thus, in the case of $\mathbf{a}_i \notin \mathcal{G}$, we have

$$p_i^* = \min_{n \in \mathcal{T}} \frac{p_n^{\max} - \sum_{l \in \mathcal{O}(n)} s_l}{\sum_{l \in \mathcal{O}(n)} q_l} \quad (44)$$

and we can express the optimal $\bar{\gamma}_i^*$ as $\bar{\gamma}_i^* = \bar{g}_i(p_i^*)$. Hence, the general solution of (34) can be expressed as

$$\bar{\gamma}_i^* = \begin{cases} \gamma_{i,\max} & \mathbf{a}_i \in \mathcal{G} \\ \bar{g}_i(p_i^*) & \text{otherwise.} \end{cases} \quad (45)$$

Note that, the proposed method for checking $\boldsymbol{\gamma}_{\min} \in \mathcal{G}$ (i.e., Algorithm 2) can be readily applied to check the condition $\mathbf{a}_i \in \mathcal{G}$ in (45) as well.

2) *Improved Upper Bounds*: Based on monotonicity of f_0 , L tighter upper bounds can be easily obtained by evaluating f_0 at the vertices of $\bar{\mathcal{Q}}^*$ adjacent to $\boldsymbol{\gamma}_{\min}$. Specifically, they are given by $f_0(\bar{\mathbf{a}}_l)$, $l \in \mathcal{L}$, where $\bar{\mathbf{a}}_l = \boldsymbol{\gamma}_{\min} + (\bar{\gamma}_l^* - \gamma_{l,\min})\mathbf{e}_l$ [see $\bar{\mathbf{a}}_1$ and $\bar{\mathbf{a}}_2$ in Figs. 4(b) and 4(c)]. Note that the values $\bar{\gamma}_l^*$, $l \in \mathcal{L}$ have already been found for computing the improved lower bound $\phi_{\text{lb}}^{\text{Imp}}(\mathcal{Q})$ (33). Let l^* be the index of the vertex which provide the best (smallest) upper bound, i.e., $l^* = \arg \min_{l \in \mathcal{L}} f_0(\bar{\mathbf{a}}_l)$. Thus, our first improved upper bound is given by

$$\phi_{\text{ub}}^{\text{Imp}}(\mathcal{Q}) = \begin{cases} f_0(\bar{\mathbf{a}}_{l^*}) & \boldsymbol{\gamma}_{\min} \in \mathcal{G} \\ 0 & \text{otherwise.} \end{cases} \quad (46)$$

¹¹Recall that we consider the nontrivial case $\mathbf{a}_i \notin \mathcal{G}$, and therefore the first inequality constraint of (34) can be safely dropped.

The following lemma ensures that $\phi_{\text{ub}}^{\text{Imp}}(\mathcal{Q})$ is tighter than the basic upper bound $\phi_{\text{ub}}^{\text{Basic}}(\mathcal{Q})$.

Lemma 4: For any $\mathcal{Q} \subseteq \mathcal{Q}_{\text{init}}$ and $\check{\boldsymbol{\gamma}} \in \mathcal{G} \cap \mathcal{Q}$ we have $\phi_{\min}(\mathcal{Q}) \leq f_0(\check{\boldsymbol{\gamma}}) \leq f_0(\boldsymbol{\gamma}_{\min}) = \phi_{\text{lb}}^{\text{Basic}}(\mathcal{Q})$.

Proof: First note from (35) that, $\phi_{\min}(\mathcal{Q}) = \inf_{\boldsymbol{\gamma} \in \mathcal{G} \cap \mathcal{Q}} f_0(\boldsymbol{\gamma})$. Moreover, by noting that $\check{\boldsymbol{\gamma}} \in \mathcal{G} \cap \mathcal{Q}$, we have $\inf_{\boldsymbol{\gamma} \in \mathcal{G} \cap \mathcal{Q}} f_0(\boldsymbol{\gamma}) \leq f_0(\check{\boldsymbol{\gamma}})$ and since $\boldsymbol{\gamma}_{\min} \preceq \check{\boldsymbol{\gamma}}$ and f_0 is monotonically decreasing in each dimension, we have $f_0(\check{\boldsymbol{\gamma}}) \leq f_0(\boldsymbol{\gamma}_{\min})$. Thus, we can combine these relations together and the result follows. ■

We can further improve the previously obtained bound by using efficient local optimization techniques. Specifically, we can use as an initial point $\boldsymbol{\gamma} = \bar{\mathbf{a}}_{l^*}$ and (locally) minimize $f_0(\boldsymbol{\gamma})$ subject to $\boldsymbol{\gamma} \in \mathcal{G} \cap \mathcal{Q}$, i.e.,

$$\begin{aligned} & \text{minimize} && f_0(\boldsymbol{\gamma}) \\ & \text{subject to} && \boldsymbol{\gamma} \in \mathcal{G} \cap \mathcal{Q}, \end{aligned} \quad (47)$$

where the variables are $\{\gamma_l\}_{l \in \mathcal{L}}$. Let us denote the obtained local optimum by $\boldsymbol{\gamma}_{\text{ImpCGP}}$. Thus, our second improved upper bound is given by

$$\phi_{\text{ub}}^{\text{ImpCGP}}(\mathcal{Q}) = \begin{cases} f_0(\boldsymbol{\gamma}_{\text{ImpCGP}}) & \boldsymbol{\gamma}_{\min} \in \mathcal{G} \\ 0 & \text{otherwise.} \end{cases} \quad (48)$$

One simple approach to compute efficiently $\boldsymbol{\gamma}_{\text{ImpCGP}}$ via complementary geometric programming (CGP) [53], is presented in Appendix B.

Since all improved bounds are tighter than the basic ones (see Lemma 3 and Lemma 4), any possible combination of a lower and an upper bound pair must also satisfy the conditions C1 and C2. This ensures the convergence of the proposed Algorithm 1.

V. EXTENSIONS TO MULTICAST NETWORKS

In this section we consider the problem of WSRMax in multicast networks [i.e., (3)] and show how Algorithm 1 can be adapted to find the solution of (3). For the sake of notational brevity, we let $\mathbf{p} = \{p_n^m\}_{n \in \mathcal{T}, m=1, \dots, M_n}$ and denote the SINR by $\text{SINR}_n^{ml}(\mathbf{p})$ [see (49) at the bottom of the page]. Thus, (3) can be expressed in the following equivalent form:

$$\begin{aligned} & \text{maximize} && \sum_{n \in \mathcal{T}} \sum_{m=1}^{M_n} \beta_n^m \log \left(1 + \min_{l \in \mathcal{O}^m(n)} \text{SINR}_n^{ml}(\mathbf{p}) \right) \\ & \text{subject to} && \sum_{m=1}^{M_n} p_n^m \leq p_n^{\max}, \quad n \in \mathcal{T} \\ & && p_n^m \geq 0, \quad n \in \mathcal{T}, \quad m = 1 \dots M_n, \end{aligned} \quad (50)$$

where the variables are p_n^m for all $n \in \mathcal{T}$ and $m = 1 \dots M_n$. The equivalence between (3) and (50) follows from the monotonically increasing property of $\log(\cdot)$ function. By introducing

$$\text{SINR}_n^{ml}(\mathbf{p}) = \frac{g_u p_n^m}{\sigma^2 + \sum_{j \in \mathcal{T}, j \neq n} \sum_{k=1}^{M_j} p_j^k \max_{i \in \mathcal{O}^k(j)} g_{il} + \sum_{k=1, k \neq m}^{M_n} p_n^k \max_{i \in \mathcal{O}^k(n)} g_{il}} \quad \text{for all } n \in \mathcal{T}, \quad m = 1, \dots, M_n. \quad (49)$$

auxiliary variables γ_n^m , $n \in \mathcal{T}$, $m = 1 \dots M_n$ we can equivalently express (50) as

$$\begin{aligned} & \text{minimize} && \sum_{n \in \mathcal{T}} \sum_{m=1}^{M_n} -\beta_n^m \log(1 + \gamma_n^m) \\ & \text{subject to} && \gamma_n^m \leq \text{SINR}_n^{ml}(\mathbf{p}), \quad n \in \mathcal{T}, m = 1 \dots M_n, \\ & && l \in \mathcal{O}^m(n) \\ & && \sum_{m=1}^{M_n} p_n^m \leq p_n^{\max}, \quad n \in \mathcal{T} \\ & && p_n^m \geq 0, \quad n \in \mathcal{T}, m = 1 \dots M_n, \end{aligned} \quad (51)$$

where the variables are p_n^m and γ_n^m for all $n \in \mathcal{T}$ and $m = 1 \dots M_n$. A close comparison of (51) and (4) reveals that they have a very similar structure. Therefore, the proposed branch and bound method (i.e., Algorithm 1) can be directly applied to solve (51) by redefining appropriately the following sets and functions:

- 1) $\gamma = \{\gamma_1, \dots, \gamma_L\}$ is replaced by $\gamma = \{\gamma_n^m\}_{n \in \mathcal{T}, m=1, \dots, M_n}$.
- 2) $f_0(\gamma)$ is replaced by $\tilde{f}_0(\gamma)$, where $\tilde{f}_0(\gamma) = \sum_{n \in \mathcal{T}} \sum_{m=1}^{M_n} -\beta_n^m \log(1 + \gamma_n^m)$.
- 3) \mathcal{G} is replaced by $\tilde{\mathcal{G}}$, where

$$\tilde{\mathcal{G}} = \left\{ \gamma \left| \begin{array}{l} \gamma_n^m \leq \text{SINR}_n^{ml}(\mathbf{p}), \quad n \in \mathcal{T}, m = 1 \dots M_n \\ l \in \mathcal{O}^m(n), \\ \sum_{m=1}^{M_n} p_n^m \leq p_n^{\max}, n \in \mathcal{T} \\ p_n^m \geq 0, \quad n \in \mathcal{T}, m = 1 \dots M_n \end{array} \right. \right\}.$$

- 4) $\mathcal{Q}_{\text{init}}$ is replaced by $\tilde{\mathcal{Q}}_{\text{init}}$, where

$$\tilde{\mathcal{Q}}_{\text{init}} = \left\{ \gamma \left| 0 \leq \gamma_n^m \leq \frac{\min_{l \in \mathcal{O}^m(n)} g_l}{\sigma^2} p_n^{\max}, n \in \mathcal{T}, m = 1, \dots, M_n \right. \right\}.$$

- 5) \mathcal{Q} is replaced by $\tilde{\mathcal{Q}}$, where $\tilde{\mathcal{Q}} = \{\gamma \mid \gamma_{n, \min}^m \leq \gamma_n^m \leq \gamma_{n, \max}^m, n \in \mathcal{T}, m = 1, \dots, M_n\}$.

Note that, the definitions of the lower and the upper bound functions provided in the case of singlecast networks [i.e., (13), (14), (33) and (46)] are applicable in the case of multicast networks as well. However, instead of the proposed efficient methods based on M-matrix theory [68, p. 112] for checking $\gamma \in \mathcal{G}$ (see Algorithm 2) and for evaluating $\tilde{\gamma}_i^*$ [see (45)], in the case of multicast networks, we have to rely on a linear programming (LP) or a GP solver.

VI. NUMERICAL EXAMPLES AND APPLICATIONS

In this section we first compare the impacts of the proposed lower bounds and upper bounds (Section IV) on the convergence of proposed branch and bound method (Algorithm 1 in Section III). Next, we provide various applications of Algorithm 1 and numerical examples for the considered applications. In summary, those applications include, sum-rate maximization in singlecast wireless networks, the problem of maximum weighted link scheduling for wireless multihop networks [17, Sec. III-B,V-A], [22, Sec. 4], cross-layer control policies for network utility maximization (NUM) in multihop wireless

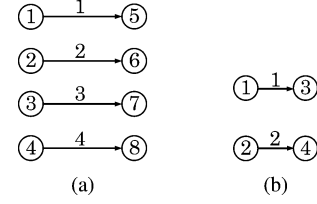


Fig. 5. (a) Bipartite network, degree 1, $N = 8$, $L = 4$. (b) Bipartite network, degree 1, $N = 4$, $L = 2$.

networks [30, Sec. 5], finding achievable rate regions in singlecast as well as in multicast wireless networks.

To simplify the presentation we use the abbreviations, LB_{Basic} for the basic lower bound given in (13), UB_{Basic} for the basic upper bound given in (14), LB_{Imp} for the improved lower bound given in (33), UB_{Imp} for the improved upper bound given in (46), and $\text{UB}_{\text{ImpCGP}}$ for the improved upper bound given in (48).

A. Impact of Different Lower Bounds and Upper Bounds on Algorithm 1

To gain insights into the impact of the proposed lower bounds and upper bounds on the convergence of Algorithm 1, we focus first to the problem of sum-rate maximization in a simple bipartite network of degree 1 [see Fig. 5(a)]. The channel power gain between distinct nodes are modeled as

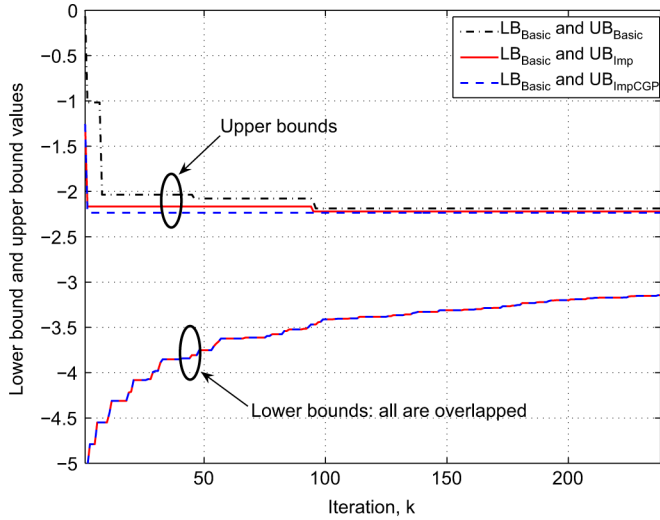
$$|h_{ij}|^2 = \mu^{|i-j|} c_{ij}, \quad i, j \in \mathcal{L}, \quad (52)$$

where c_{ij} s are small-scale fading coefficients and the scalar $\mu \in [0, 1]$ is referred to as interference coupling index which parameterizes the interference between direct links. The fading coefficients are assumed to be exponentially distributed independent random variables to model Rayleigh fading. An arbitrarily generated set \mathcal{C} of fading coefficients where $\mathcal{C} = \{c_{ij} \mid i, j \in \mathcal{L}\}$ is referred to as a *single fading realization*. We define the signal-to-noise ratio (SNR) operating point as $(p_n^{\max} = p_0^{\max})$ for all $n \in \mathcal{T}$

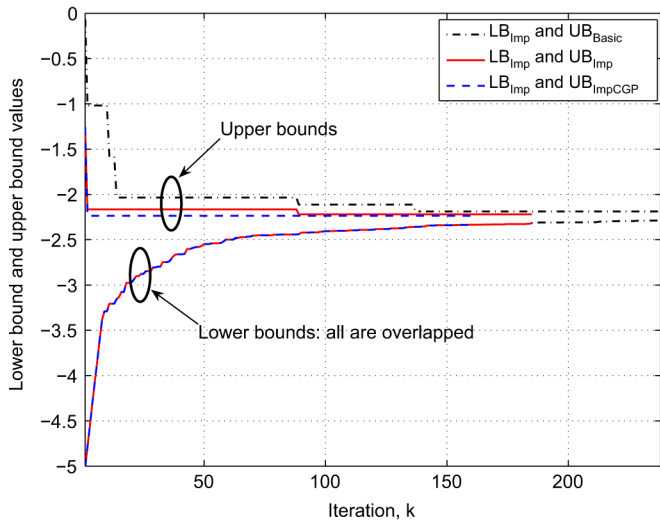
$$\text{SNR} = \frac{p_0^{\max}}{\sigma^2}. \quad (53)$$

We consider first the nonfading case, i.e., $c_{ij} = 1, i, j \in \mathcal{L}$ and the proposed Algorithm 1 was run with all possible combinations of the proposed lower and upper bound pairs. Fig. 6 shows the evolution of upper and lower bounds for the optimal value of (4)¹² for $\text{SNR} = 15$ dB, $\mu = 0.25$, and $\beta_l = 0.25$ for all $l \in \mathcal{L}$. Specifically in Fig. 6(a), we used the basic lower bound LB_{Basic} in conjunction with all proposed upper bounds and in Fig. 6(b) we used the improved lower bound LB_{Imp} in conjunction with all proposed upper bounds. The results show that the convergence speed of Algorithm 1 can be substantially increased by improving the lower bound whilst the tightness of the upper bound has a much reduced impact. Note that this is in general the behavior of a branch and bound method, where an approximative solution can be found relatively fast but certifying it takes typically much larger number of iterations [49]. Note that in both Fig. 6(a) and (b) the evolution of lower bounds is independent on the upper bound used. This is due to the fact

¹²The optimal value of (4) is the negative of the optimal value of (2).



(a)

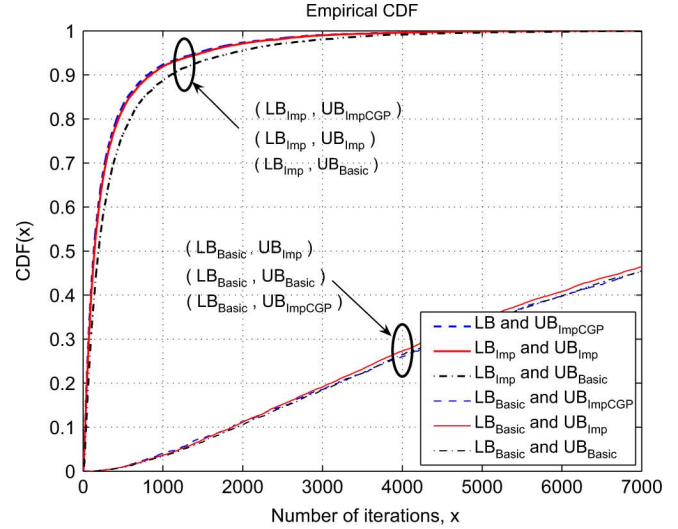


(b)

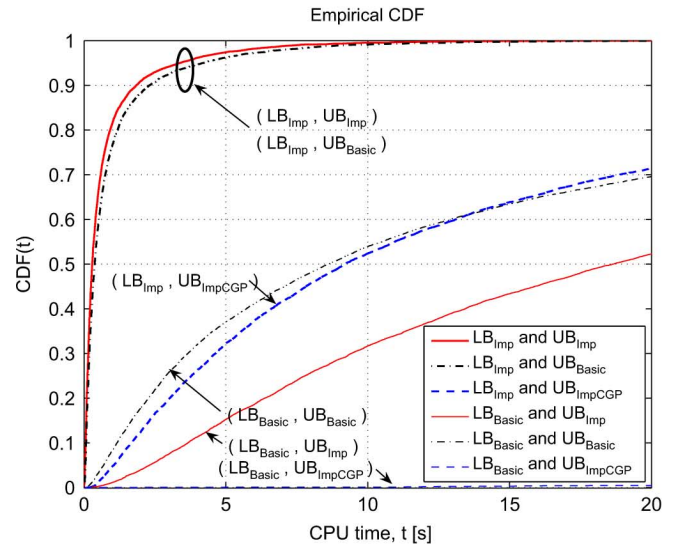
Fig. 6. Evolution of lower and upper bounds: (a) Basic lower bound in conjunction with all upper bounds; (b) Improved lower bound in conjunction with all upper bounds.

that in each iteration the branching mechanism depends only on the lower bound.

In order to provide a statistical description for the speed of convergence we turn to the fading case and run Algorithm 1 for a large number of fading realizations. For each one we store the number of iterations and the total CPU time required to find the optimal value of (4) within an accuracy of $\epsilon = 10^{-1}$ for SNR = 15 dB, $\mu = 0.25$, and $\beta_l = 0.25$ for all $l \in \mathcal{L}$. Fig. 7 shows the empirical cumulative distribution function (CDF) plots of total number of iterations [Fig. 7(a)] and total CPU time [Fig. 7(b)] for all possible combinations of lower and upper bounds pairs. Fig. 7(a) shows that, irrespective of the upper bound we use, the improved lower bound LB_{Imp} provides remarkable reduction in total number of iterations as compared to LB_{Basic} . Results further show that, even though, the improved upper bound UB_{ImpCGP} makes use of advanced optimization techniques such as complementary geometric programming (CGP) (see Algorithm 3, Appendix B), the benefits



(a)



(b)

Fig. 7. Empirical CDF plots of: (a) total number of iterations; (b) total CPU time.

from UB_{ImpCGP} over the improved upper bound UB_{Imp} is marginal in terms of total number of iterations. In terms of total CPU time [Fig. 7(b)], significant improvements often are achieved by using the lower and upper bound pairs (LB_{Imp}, UB_{Imp}) and (LB_{Imp}, UB_{Basic}) . Interestingly, the lower and upper bound pair (LB_{Imp}, UB_{ImpCGP}) performs very poorly. This behavior is due to the complexity of Step 2 of Algorithm 3, where we have to rely on a GP solver.

Therefore, in all of the following numerical examples, Algorithm 1 is run with the lower and upper bound pair (LB_{Imp}, UB_{Imp}) , unless otherwise specified.

B. Sum-Rate Maximization in Singlecast Wireless Networks

Let us now consider the problem of sum-rate maximization in a bipartite singlecast network. To evaluate the benefits from multipacket transmit/receive capabilities of nodes, we chose a network setup with degree 3 as shown in Fig. 8. The network is symmetric and the distances between nodes are chosen as shown

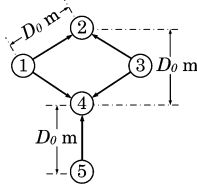


Fig. 8. Bipartite network, degree 3, $N = 5$, $L = 5$.

in the figure. We assume an exponential path loss model, where the channel power gains between distinct nodes are given by

$$|h_{ij}|^2 = \left(\frac{d_{ij}}{d_0}\right)^{-\eta} c_{ij}, \quad (54)$$

where d_{ij} is the distance from the transmitter of link i to the receiver of link j , d_0 is the *far field reference distance* [70], η is the path loss exponent, and c_{ij} are defined similarly as in (52). Note that, the interference coefficients g_{ij} s are chosen as we discussed in Section II. The first term of (54) represents the path loss factor and the second term models the Rayleigh small-scale fading. The SNR operating point is defined as ($p_n^{\max} = p_0^{\max}$ for all $n \in \mathcal{T}$)

$$\text{SNR} = \frac{p_0^{\max}}{\sigma^2} \cdot \left(\frac{D_0}{d_0}\right)^{-\eta}. \quad (55)$$

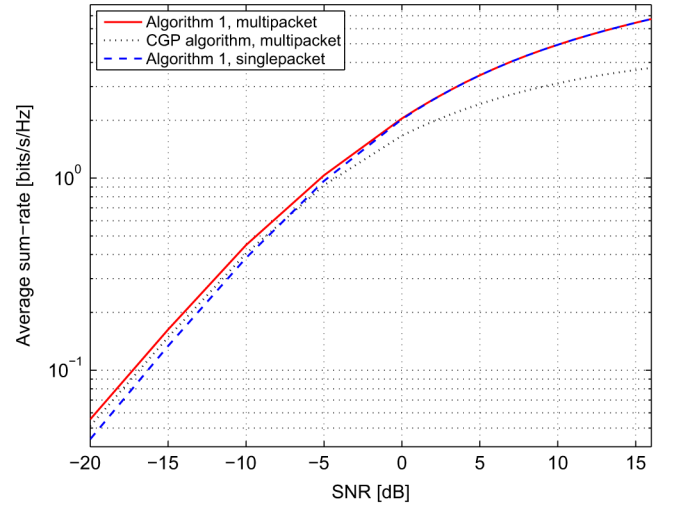
In the following simulations we set $\frac{D_0}{d_0} = 10$ and $\eta = 4$.

Fig. 9(a) shows the dependence of average sum-rate¹³ on the SNR. Results show that, the average sum-rate in the case of multipacket transmission/reception is always better than or equal to the case of singlepacket transmission/reception and the performance gap increases as SNR decreases. However, as expected for practical SNR values, the benefits of multipacket transmission/reception are negligible when the receivers perform singleuser detection [2]. For comparison, we also plot the result obtained from a suboptimal solution method based on complementary geometric programming (CGP) [53]–[55]. We refer to this suboptimal method as *CGP algorithm* in the rest of the paper. Note that, CGP algorithm is equivalent to running Algorithm 3 (Appendix B) with $Q = Q_{\text{init}}$ and a proper initialization $\hat{\gamma}$. Specifically, we found the initial $\hat{\gamma}_l$, $l \in \mathcal{L}$ according to (29) by using a uniform feasible power allocation which will be referred to as uniform initialization in the rest of the paper. Let us first focus to the CGP performance in the case of multipacket transmission/reception. Results show that, there is a significant performance loss due to the suboptimality of CGP algorithm, especially for $\text{SNR} > 0$ dB. In the case of singlepacket transmission/reception, the average sum-rate that is obtained by using CGP algorithm is almost zero irrespective of the SINR and not plotted in Fig. 9(a) to preserve the clarity. Results confirm that, CGP algorithm can not handle huge imbalance between interference coefficient values.¹⁴

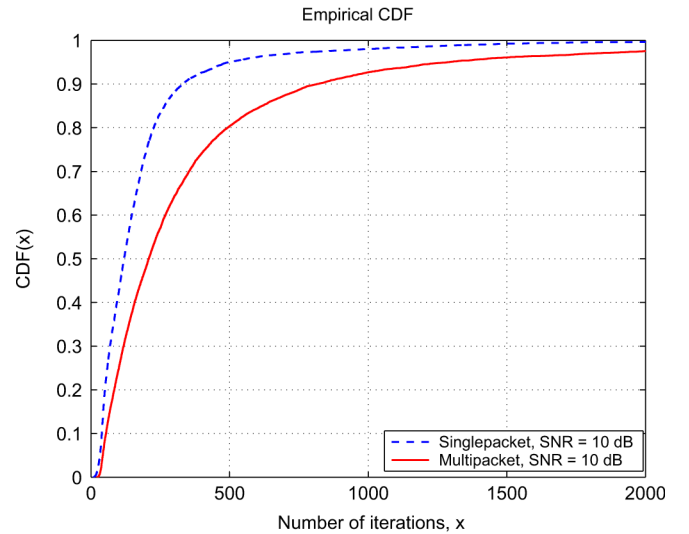
Fig. 9(b) shows the empirical CDF plots of total number of iterations required to find the sum-rate by using Algorithm 1, which gives insight into the complexity of Algorithm 1. The plots are for the case of $\text{SNR} = 10$ dB and $\epsilon = 10^{-3}$. Roughly

¹³That is, $\beta_l = 1$ for all $l \in \mathcal{L}$

¹⁴Recall from Fig. 2(a) and (b) that, if nodes have singlepacket transmitter/receiver capabilities, then some of the interference coefficients are infinite.



(a)



(b)

Fig. 9. (a) Dependence of average sum-rate on SNR; (b) Empirical CDF of total number of iterations.

speaking, results show that the total number of iterations required in the case of singlepacket transmission/reception is smaller as compared to the case of multipacket transmission/reception.

C. Maximum Weighted Link Scheduling in Multihop Wireless Networks

Next, we consider a multihop wireless network, where the nodes have only singlepacket transmit/receive capability and no node can transmit and receive simultaneously. In such setups WSRMax problem is equivalent to the maximum weighted matching¹⁵ (MWM) problem [27]. Polynomial time algorithms are available for the problem in the case of fixed link rates [27], [22, Sec. 4.2]. To the best of our knowledge, there are no known solution methods for MWM problem when the link rates depend on the power allocation of all other links. In such cases, it is worth noting that, our proposed algorithm is able to find the maximum weighted matching.

¹⁵Borrowing terminology from the graph theory, a matching is a set of links, no two of which share a node [27]

TABLE I
MAXIMUM WEIGHTED MATCHINGS

| Associated weights of the links \ SNR [dB] | -10 | 0 | 5 | 10 |
|--|-----|---|---|----|
| | | | | |
| | | | | |
| | | | | |

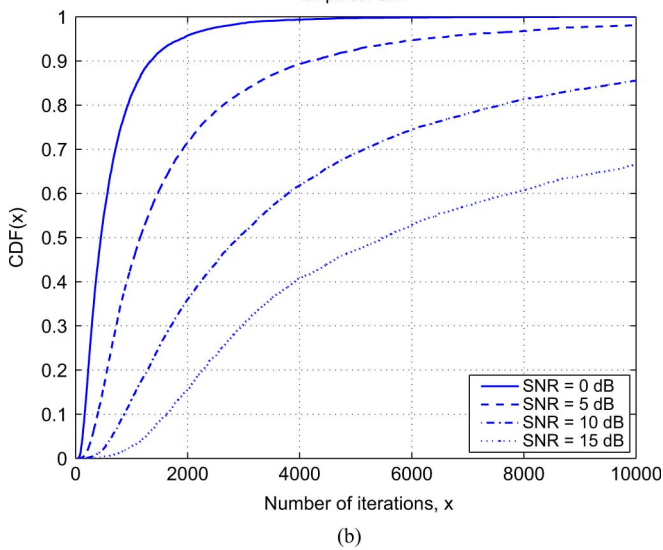
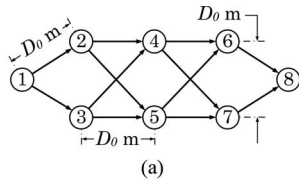


Fig. 10. (a) Multihop network, $N = 8, L = 12$; (b) Empirical CDF of total number of iterations.

To show this, we use the symmetric multihop wireless network shown in Fig. 10(a). The channel power gains, between nodes are given by (54) and the SNR operating point is given by (55). In the following simulations we set $\frac{D_0}{d_0} = 10$ and $\eta = 4$.

Table I shows maximum weighted matchings obtained for different link weights (see the left most column) and the SNR combinations in the case of no fading, i.e., $c_{ij} = 1, i, j \in \mathcal{L}$. Results show that, the smaller the SNR, the larger the number of links that are activated simultaneously in the maximum weighted matching. This is intuitively expected since, at low SNR values, node transmission power is small, and therefore the interference generated is very small so that many links are activated simultaneously.

To gain some insight into the computational complexity of the algorithm we plot the CDF of total number of iterations by running the algorithm for a large number of fading realizations.

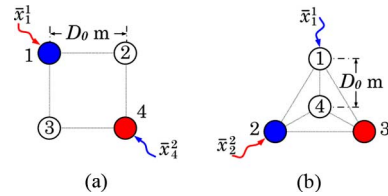


Fig. 11. (a) Multihop network 1, $N = 4$, fully connected, $S = 2$; (b) Multihop network 2, $N = 4$, fully connected, $S = 2$.

Fig. 10(b) shows the empirical CDF plots of total number of iterations required to terminate Algorithm 1 (or to find the maximum weighted matching). Plots are drawn for the cases of SNR = 0, 5, 10, and 15 dB, $\beta_l = 1$ for all $l \in \mathcal{L}$, and $\epsilon = 10^{-2}$. Results show that, the smaller the SNR, the smaller the total number of iterations required to find the maximum weighted matching. For example, In the case of SNR = 0 dB, with probability 0.9, the maximum weighted matching is found in less than 1500 iterations. However, in the case of SNR = 5 dB, with the same probability 0.9, the maximum weighted matching is found in less than 4000 iterations.

D. Cross-Layer Control Policies for NUM in Multihop Wireless Networks

In this section we specifically consider the problem of network utility maximization subject to stability constraints [30, Sec. 5]. Let us first revisit briefly the commodity description of the network. Exogenous data arrives at the source nodes and they are delivered to the destination nodes over several, possibly multi-hop, paths. We identify the data by their destinations, i.e., all data with the same destination are considered as a single commodity, regardless of its source. We label the commodities with integers $s = 1, \dots, S$ ($S \leq N$). For every node, we define $\mathcal{S}_n \subseteq \{1, \dots, S\}$ as the set of commodities which can arrive exogenously at node n . The network is time slotted and at each source node, a set of flow controllers decides the amount of each commodity data admitted every time slot in the network. Let $x_n^s(t)$ denote the amount of data of commodity s admitted in the network at node n during time slot t . It is assumed that the data which is successfully delivered to its destination exits the network layer. Associated with each node-commodity pair $(n, s)_{s \in \mathcal{S}_n}$ we define a concave and nondecreasing utility function $g_n^s(y)$, representing the “reward” received by sending data of commodity s from node n to node d_s at a long term average

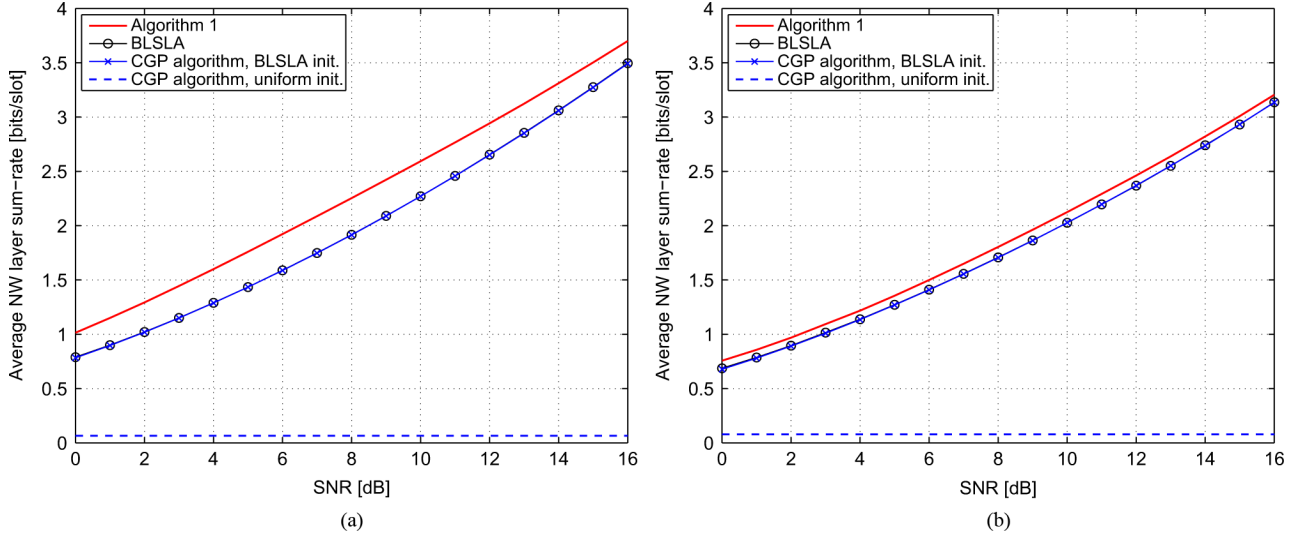


Fig. 12. (a) Dependence of average NW layer sum-rate on SNR for network 1; (b) Dependence of average NW layer sum-rate on SNR for network 2.

rate of y [bits/slot]. Thus, the NUM problem under stability constraints can be formulated as [30, Sec. 5]

$$\begin{aligned} & \text{maximize} && \sum_{n \in \mathcal{T}} \sum_{s \in \mathcal{S}_n} g_n^s(y_n^s) \\ & \text{subject to} && \{y_n^s | n \in \mathcal{T}, s \in \mathcal{S}_n\} \in \mathbf{\Lambda}, \end{aligned} \quad (56)$$

where the optimization variables are y_n^s and $\mathbf{\Lambda}$ represents the *network layer capacity region* [30, Def. 3.7].

An arbitrarily close to optimal solutions for (56) is achieved by a cross-layer control policy which consists of solving three subproblems: 1) flow control; 2) next-hop routing and in-node scheduling; and 3) resource allocation (RA), during each time slot [30]. The RA subproblem exactly resembles the weighted sum-rate maximization problem (2) where the weights are given by the maximum differential backlogs of network links [30]. Here, we implement the cross-layer control algorithm in [30] and, in the third step, we use our proposed Algorithm 1 to solve the RA subproblem. The cross-layer control algorithm is simulated for at least $T = 10000$ time slots and the average rates \bar{x}_n^s are computed by averaging the last $t_0 = 3000$ time slots, i.e., $\bar{x}_n^s = \frac{1}{t_0} \sum_{t=T-t_0}^T x_n^s(t)$. We assume that the average rates \bar{x}_n^s corresponding to all node-commodity pairs $(n, s)_{s \in \mathcal{S}_n}, n \in \mathcal{N}$ are subject to proportional fairness and therefore we select the utility functions $g_n^s(\bar{x}_n^s) = \ln(\bar{x}_n^s)$. Detail descriptions of the cross-layer control policy is beyond the scope of this paper and the reader may refer to [30] for more explanations.

Two fully connected multihop wireless network setups as shown in Fig. 11 are considered, where all nodes have multi-packet transmit/receive capability and any node can not transmit and receive simultaneously. Each of the network consist of four nodes (i.e., $N = 4$) and two commodities which arrive exogenously at source nodes. In the case of first network setup shown in Fig. 11(a), commodity 1 arrives exogenously at node 1 and is intended for node 4; commodity 2 arrives exogenously at node 4 and is intended for node 1. Nodes are located in a square grid such that the horizontal and the vertical distance between adjacent nodes are D_0 meters [m]. In the case of second network setup shown in Fig. 11(b), commodity 1 arrives

exogenously at node 1 and is intended for node 2; commodity 2 arrives exogenously at node 2 and is intended for node 3. Nodes are located such that, three of them form an equilateral triangle and the fourth one is located at its center [see Fig. 11(b)]. It is assumed that, the distance from the middle node to any other is D_0 m. The channel power gains are given by (54) and SNR operating point is given by (55). We set $\frac{D_0}{d_0} = 10$ and $\eta = 4$ in the following simulation.

Fig. 12 shows the dependence of the average NW layer sum-rate on the SNR for the considered network setups. As a references, we first consider a suboptimal and more restrictive RA policy, where only one link can be activated during each time slot. This policy is called base line single link activation (BLSLA).¹⁶ Other suboptimal RA policy is based on CGP algorithm (see Section VI-B). Specifically, we use two initialization methods for CGP algorithm: 1) the initial $\hat{\gamma}_l, l \in \mathcal{L}$ is found according to (29) by using BLSLA power allocation, 2) the uniform initialization as discussed in Section VI-B.

Results show that, the gains obtained by using Algorithm 1 are always larger as compared to other suboptimal methods. The relative gains achieved by Algorithm 1 in the case of network setup 2 [Fig. 12(a)] is more significant than in the case of network setup 3 [Fig. 12(b)]. Results further show that, the suboptimal CGP algorithm is very sensitive to the initialization. For example, in the case of uniform initialization, CGP algorithm performs extremely poorly as compared to the case of BLSLA based initialization. Moreover, in the case of BLSLA based initialization, the suboptimal CGP algorithm can not perform beyond the limits that are achieved by simple BLSLA RA policy.

E. Achievable Rate Regions in Singlecast (SC) Wireless Networks

In this section we illustrate how the Algorithm 1 can be used to find the achievable rate region in singlecast wireless networks. Recall that, we consider the case where all receiver nodes perform singleuser detection, and therefore the achievable rate regions we are referring to are different from the information

¹⁶BLSLA policy can be easily found and it consists of activating during each time slot only the link which achieves the maximum weighted rate

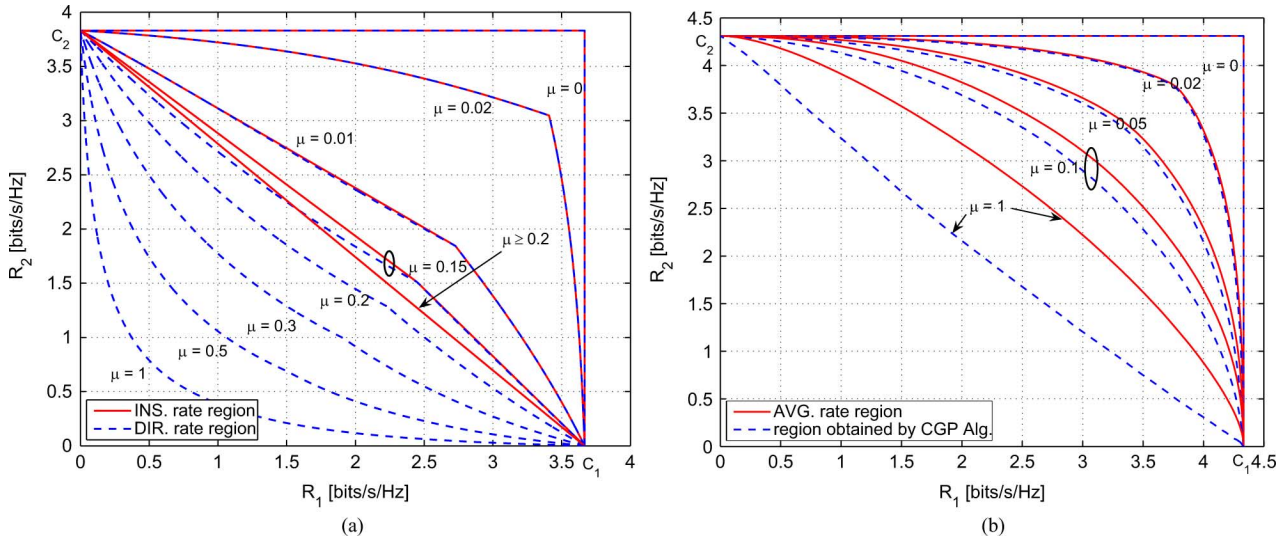


Fig. 13. Rate regions: (a) Directly achievable and instantaneous rate regions; (b) Average rate regions.

theoretic capacity regions[71]–[73]. Note that, information theoretic capacity region is not known even for the simple case of two interfering links[74].

To facilitate the graphical illustration, we consider a simple bipartite singlecast network of degree 1 as shown in Fig. 5(b). The channel power gains are given by (52) and the SNR operating point is given by (53).

We start by defining the *directly achievable rate region*, the *instantaneous rate region*, and the *average rate region* for singlecast wireless networks. Let $\mathcal{R}^{\text{DIR-SC}}(\mu, C^t, p_1^{\max}, p_2^{\max})$ denote the directly achievable rate region for a given interference coupling index μ , a given fading realization $C^t = \{c_{11}^t, c_{12}^t, c_{22}^t, c_{21}^t\}$, and maximum node transmission power p_1^{\max} and p_2^{\max} , i.e.,

$$\mathcal{R}^{\text{DIR-SC}}(\mu, C^t, p_1^{\max}, p_2^{\max}) = \left\{ (R_1, R_2) \left| \begin{array}{l} R_1 \leq \log \left(1 + \frac{c_{11}^t p_1}{\sigma^2 + \mu c_{21}^t p_2} \right) \\ R_2 \leq \log \left(1 + \frac{c_{22}^t p_2}{\sigma^2 + \mu c_{12}^t p_1} \right) \\ 0 \leq p_1 \leq p_1^{\max}, \quad 0 \leq p_2 \leq p_2^{\max} \end{array} \right. \right\}. \quad (57)$$

By invoking a time sharing argument, one can obtain the instantaneous rate region $\mathcal{R}^{\text{INS-SC}}(\mu, C^t, p_1^{\max}, p_2^{\max})$ which is the convex hull of $\mathcal{R}^{\text{DIR-SC}}(\mu, C^t, p_1^{\max}, p_2^{\max})$. That is,

$$\mathcal{R}^{\text{INS-SC}}(\mu, C^t, p_1^{\max}, p_2^{\max}) = \text{conv} \{ \mathcal{R}^{\text{DIR-SC}}(\mu, C^t, p_1^{\max}, p_2^{\max}) \},$$

where $\text{conv}\{\mathcal{R}\}$ denotes the convex hull of the set \mathcal{R} . As noted in [75], since the instantaneous rate region $\mathcal{R}^{\text{INS-SC}}(\mu, C^t, p_1^{\max}, p_2^{\max})$ is convex, any boundary point of the rate region can be obtained by using the solution of an optimization problem in the form of (2) with $\beta_1 = \alpha, \beta_2 = (1 - \alpha)$ for some $\alpha \in [0, 1]$.

Finally, we define the average rate region $\mathcal{R}^{\text{AVE-SC}}(\mu, p_1^{\max}, p_2^{\max})$ for a given interference coupling index μ and a maximum node transmission power p_1^{\max} and p_2^{\max} as $\mathcal{R}^{\text{AVE-SC}}(\mu, p_1^{\max}, p_2^{\max}) = \frac{1}{T} \sum_{t=1}^T \mathcal{R}^{\text{INS-SC}}(\mu, C^t, p_1^{\max}, p_2^{\max})$, where addition and

scalar multiplication of sets is used.¹⁷ The nonnegative integer T is the total number of fading realizations we used in averaging. Note that, any boundary point $[R_1^b, R_2^b]^T$ of $\mathcal{R}^{\text{AVE-SC}}(\mu, p_1^{\max}, p_2^{\max})$ is obtained by using the following steps for some $\alpha \in [0, 1]$: 1) solve (2) with $\beta_1 = \alpha$ and $\beta_2 = 1 - \alpha$ for T fading realizations, 2) for each fading realization $t \in \{1, \dots, T\}$, evaluate the rate of link 1 and 2 denoted by r_1^t, r_2^t according to (1), and 3) average r_1^t and r_2^t over all T fading realizations to obtain $R_1^b = \frac{1}{T} \sum_{t=1}^T r_1^t$ and $R_2^b = \frac{1}{T} \sum_{t=1}^T r_2^t$.

Fig. 13(a) shows the instantaneous rate regions $\mathcal{R}^{\text{INS-SC}}(\mu, C^t, p_1^{\max}, p_2^{\max})$ for different values of μ and for an arbitrary chosen fading realization in the case of SNR = 15 dB. Specifically, the fading coefficients are $c_{11} = 0.4185, c_{12} = 0.3421, c_{22} = 0.3700$, and $c_{21} = 1.299$. As a reference we also plot the directly achievable rate regions $\mathcal{R}^{\text{DIR-SC}}(\mu, C^t, p_1^{\max}, p_2^{\max})$ for all the scenarios considered.¹⁸ Results show that, the smaller the μ , the larger the rate regions. This is intuitively explained by noting that, the smaller the μ , the smaller the interference coefficients, g_{ij} between links, and therefore higher the rates. Results further show that, when $\mu \geq 0.2$, the directly achievable rate regions become nonconvex, whereas the instantaneous rate region is a triangle referred to as time division multiple access (TDMA) rate region obtained by time sharing between the maximum rates of R_1 and R_2 . Moreover, when $\mu < 0.2$, instantaneous rate region expands beyond the TDMA rate region and for $\mu \leq 0.01$, the directly achievable rate region almost overlaps with the instantaneous rate region.

Fig. 13(b) shows the average rate region $\mathcal{R}^{\text{AVE-SC}}(\mu, p_1^{\max}, p_2^{\max})$ for different values of μ in the case of SNR = 15 dB. As a reference, we also plot the region obtained by using CGP algorithm to (2). Results show that, the region obtained by CGP algorithm is always worse

¹⁷For vector sets \mathcal{A} and \mathcal{B} and scalars α, β , the set $\alpha\mathcal{A} + \beta\mathcal{B}$ is defined as $\{\alpha\mathbf{a} + \beta\mathbf{b} \mid \mathbf{a} \in \mathcal{A}, \mathbf{b} \in \mathcal{B}\}$ [66, p. 38]

¹⁸The problem of finding any boundary point of $\mathcal{R}^{\text{DIR-SC}}(\mu, C^t, p_1^{\max}, p_2^{\max})$ can be easily cast as a GP or as a problem of the form (34).

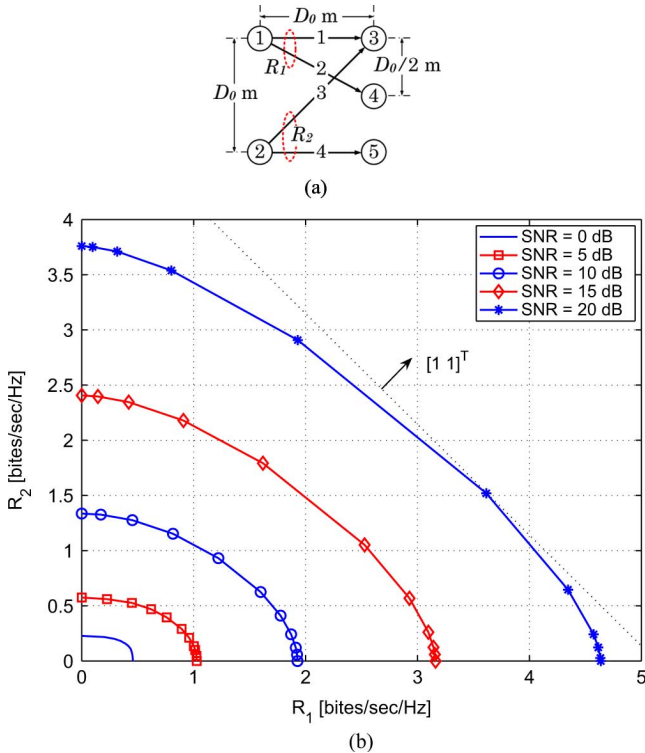


Fig. 14. (a) Multicast network, $\mathcal{T} = \{1, 2\}$, $M_1 = 1$, $M_2 = 1$, $\mathcal{O}^1(1) = \{1, 2\}$, $\mathcal{O}^1(2) = \{3, 4\}$; (b) Average rate region.

than the average rate region. The gap in the performance is more pronounced in the case of larger values of μ . Note that, even in the case of $\mu = 1$, the average rate region is bounded by a concave function with end points C_1 and C_2 , although, the corresponding instantaneous rate regions used in the averaging are triangles [see Fig. 13(a)] in general. This phenomenon is due to the property of the set addition used in the definition of $\mathcal{R}^{\text{AVE-SC}}(\mu, p_1^{\max}, p_2^{\max})$. Results also show that, the smaller the μ , the larger the average rate region.

F. Achievable Rate Regions in Multicast (MC) Wireless Networks

We finally show the applicability of Algorithm 1 for finding the rate regions in a multicast wireless networks. A multicast with only two multicast transmissions [see Fig. 14(a)] is considered for the sake of graphical illustration of the rate regions. Node 1 has common information to be sent to node 3 and 4, whereas node 2 has common information to be sent to node 3 and 5. We assume that node 3 has multipacket receiver capability. The channel power gains are given by (54) and SNR operating point is given by (55). Moreover, we set $\frac{D_0}{d_0} = 10$ and $\eta = 4$.

As in the case of singlecast wireless networks, we first define the directly achievable rate region, instantaneous rate region, and the average rate region for multicast wireless networks. Particularized to the network setup considered in Fig. 14(a), for a given set of interference coefficients $G^t = \{g_{11}^t, g_{22}^t, g_{33}^t, g_{44}^t, g_{14}^t, g_{32}^t\}$ and maximum node transmission power p_1^{\max} and p_2^{\max} , the instantaneous rate region $\mathcal{R}^{\text{INS-MC}}(G^t, p_1^{\max}, p_2^{\max})$ is defined as $\mathcal{R}^{\text{INS-MC}}(G^t, p_1^{\max}, p_2^{\max}) = \text{conv}\{\mathcal{R}^{\text{DIR-MC}}(G^t,$

$p_1^{\max}, p_2^{\max})\}$, where $\mathcal{R}^{\text{DIR-MC}}(G^t, p_1^{\max}, p_2^{\max})$ denotes the directly achievable rate region for multicast wireless networks, i.e.,

$$\mathcal{R}^{\text{DIR-MC}}(G^t, p_1^{\max}, p_2^{\max}) = \left\{ (R_1, R_2) \left[\begin{array}{l} R_1 \leq \log \left(1 + \frac{g_{11}^t p_1^1}{\sigma^2 + g_{33}^t p_2^1} \right) \\ R_1 \leq \log \left(1 + \frac{g_{22}^t p_1^1}{\sigma^2 + g_{32}^t p_2^1} \right) \\ R_2 \leq \log \left(1 + \frac{g_{33}^t p_2^1}{\sigma^2 + g_{11}^t p_1^1} \right) \\ R_2 \leq \log \left(1 + \frac{g_{44}^t p_2^1}{\sigma^2 + g_{14}^t p_1^1} \right) \\ 0 \leq p_1^1 \leq p_1^{\max}, 0 \leq p_2^1 \leq p_2^{\max} \end{array} \right. \right\}. \quad (58)$$

Finally, for a given maximum node transmission power p_1^{\max} and p_2^{\max} , the average rate region $\mathcal{R}^{\text{AVE-MC}}(p_1^{\max}, p_2^{\max})$ is defined as $\mathcal{R}^{\text{AVE-MC}}(p_1^{\max}, p_2^{\max}) = \frac{1}{T} \sum_{t=1}^T \mathcal{R}^{\text{INS-MC}}(G^t, p_1^{\max}, p_2^{\max})$.

Fig. 14(b) shows the average multicast rate region for different SNR values. Results show that, when the weights associated with rates R_1 and R_2 are the same, the resulting R_1 is always greater than R_2 . For example, in the case of SNR = 20 dB, we have $R_1 = 3.71$ bits/s/Hz and $R_2 = 1.50$ bits/s/Hz. Roughly speaking, this observation can be explained as follows: R_1 is determined by the rate of links 2 (the weakest of link 1 and 2), R_2 is determined by the rate of links 3 (the weakest of link 3 and 4) and rate of link 2 is larger than that of link 3 due to path losses.

VII. CONCLUSION

We have considered the problem of weighted sum-rate maximization (WSRMax) for a set of interfering links. In fact, this problem is NP-hard. A solution method, based on the branch and bound technique has been proposed for solving the non-convex WSRMax problem globally with an optimality certificate. Efficient and analytic bounds were proposed and their impact on the convergence were numerically evaluated. The convergence speed of the proposed algorithm can be substantially increased by improving the lower bound whilst the tightness of the upper bound has a much reduced impact. Numerical results showed that the proposed algorithm converged fairly fast in all considered setups. Nevertheless, since the problem is NP-hard, the worst case complexity can be exponential in the number of variables. The considered link-interference model is fairly general so that it can model a wide range of network topologies with various node capabilities such as single- or multi-packet transmission (or reception) and simultaneous transmission and reception. Unlike other branch and bound based solution methods for WSRMax, our method does not require the problem to be convertible into a DC (difference of convex functions) problem. Therefore, the proposed method applies to a broader class of WSRMax problems (e.g., WSRMax in multicast wireless networks). Moreover, the method proposed can also be used to maximize any system performance metric that can be expressed as a Lipschitz continuous and increasing function of SINR values and is not restricted to WSRMax. Given its generality, the proposed algorithm can be adapted to address a wide range of network control and optimization problems. Performance benchmarks for various network topologies

can be obtained by back-substituting it into any network design method which relies on WSRMax. Several applications, including cross-layer network utility maximization and maximum weighted link scheduling for multihop wireless networks as well as finding achievable rate regions for singlecast/multicast wireless networks, have been presented. As suboptimal but less complex algorithms are typically used in practice, the proposed algorithm can also be used for evaluating their performance loss.

APPENDIX A
PROOF OF THEOREM 2

Theorem 2 shows certain similarities to the classical feasibility conditions derived in [76]–[79]. These conditions were derived based on Perron-Frobenius theory [80] by assuming the primitiveness of $\mathbf{B}(\boldsymbol{\gamma})\mathbf{G}$. We give a slightly more general proof based on the theory of M-matrices [68, p. 112] which circumvent the technical condition of $\mathbf{B}(\boldsymbol{\gamma})\mathbf{G}$ being primitive. Thus they hold for any nonnegative matrix $\mathbf{B}(\boldsymbol{\gamma})\mathbf{G}$.

To prove the first statement we show that $\rho(\mathbf{B}(\boldsymbol{\gamma})\mathbf{G}) < 1$ is necessary for $\boldsymbol{\gamma} \in \mathcal{G}$. Recall that, (29) can be expressed as $\mathbf{A}(\boldsymbol{\gamma})\mathbf{p} \succeq \mathbf{b}(\boldsymbol{\gamma})$. Thus, we can write the following necessary (but not sufficient) condition for $\boldsymbol{\gamma} \in \mathcal{G}$:

$$\boldsymbol{\gamma} \in \mathcal{G} \Rightarrow \exists \mathbf{p} \succeq \mathbf{0} \text{ such that } \mathbf{A}(\boldsymbol{\gamma})\mathbf{p} \succeq \mathbf{b}(\boldsymbol{\gamma}). \quad (\text{A.1})$$

The condition above is easily derived by ignoring the second set of inequalities (i.e., the power constraints) in the description of \mathcal{G} in (5). Strict positivity of $\boldsymbol{\gamma}$ implies that $\mathbf{b}(\boldsymbol{\gamma}) \succ \mathbf{0}$ and $\mathbf{p} \succ \mathbf{0}$. This observation together with (A.1) yield the following necessary conditions for $\boldsymbol{\gamma} \in \mathcal{G}$:

$$\boldsymbol{\gamma} \in \mathcal{G} \Rightarrow \exists \mathbf{p} \succ \mathbf{0} \text{ such that } \mathbf{A}(\boldsymbol{\gamma})\mathbf{p} \succ \mathbf{0}. \quad (\text{A.2})$$

Finally, [68, Th. 2.5.3, items 12 and 2] states that $\exists \mathbf{p} \succ \mathbf{0}$ such that $\mathbf{A}(\boldsymbol{\gamma})\mathbf{p} \succ \mathbf{0}$ if and only if $\rho(\mathbf{B}(\boldsymbol{\gamma})\mathbf{G}) < 1$. Consequently, we can rewrite (A.2) equivalently as $\boldsymbol{\gamma} \in \mathcal{G} \Rightarrow \rho(\mathbf{B}(\boldsymbol{\gamma})\mathbf{G}) < 1$ which, by the contraposition, is equivalent to $\rho(\mathbf{B}(\boldsymbol{\gamma})\mathbf{G}) \geq 1 \Rightarrow \boldsymbol{\gamma} \notin \mathcal{G}$.

The second part follows directly from the description of \mathcal{G} in (5), where the SINR constraints (29) are satisfied with equality, i.e., $\mathbf{A}(\boldsymbol{\gamma})\mathbf{p} = \mathbf{b}(\boldsymbol{\gamma})$. Note that since the nonnegative matrix $\mathbf{B}(\boldsymbol{\gamma})\mathbf{G}$ has the spectral radius smaller than one, i.e., $\rho(\mathbf{B}(\boldsymbol{\gamma})\mathbf{G}) < 1$, the matrix $\mathbf{A}(\boldsymbol{\gamma}) = \mathbf{I} - \mathbf{B}(\boldsymbol{\gamma})\mathbf{G}$ is invertible and its inverse has nonnegative entries, i.e., $\mathbf{A}^{-1}(\boldsymbol{\gamma}) \succeq \mathbf{0}$ [68, Th. 2.5.3, items 2 and 17]. Thus $\mathbf{p} = \mathbf{A}^{-1}(\boldsymbol{\gamma})\mathbf{b}(\boldsymbol{\gamma}) \succeq \mathbf{0}$.

We prove the third part by showing that $\mathbf{p}^* = \mathbf{A}^{-1}(\boldsymbol{\gamma})\mathbf{b}(\boldsymbol{\gamma})$ is the minimum power vector¹⁹ (with respect to generalized inequality $\preceq_{\mathbb{R}_+^L}$) which satisfy the SINR constraints in (29), i.e., \mathbf{p}^* is the unique solution of the following vector optimization problem²⁰

$$\begin{aligned} & \text{minimize (w.r.t. } \mathbb{R}_+^L) && \mathbf{p} \\ & \text{subject to } && \mathbf{A}(\boldsymbol{\gamma})\mathbf{p} \succeq \mathbf{b}(\boldsymbol{\gamma}), \end{aligned} \quad (\text{A.3})$$

¹⁹A point $\mathbf{p} \in \mathcal{S}$ is the minimum element of set \mathcal{S} w.r.t generalized inequality $\preceq_{\mathbb{R}_+^L}$ if and only if $\mathcal{S} \subset \mathbf{p} + \mathbb{R}_+^L$ [66, Sec. 2.4.2].

²⁰We refer the reader to [66, Sec. 4.7], where a detailed discussion of vector optimization is presented.

where the optimization variables are $p_l, l \in \mathcal{L}$. Since \mathbf{p}^* is the minimum power vector that achieves SINR values $\boldsymbol{\gamma}$, if it violates any power constraint then any other power vector \mathbf{p} that achieves $\boldsymbol{\gamma}$ must also violate those power constraints, because $\mathbf{p}^* \preceq \mathbf{p}$.

A standard technique for solving vector optimization problems is scalarization [66, Sec. 4.7.4]. We choose an arbitrary $\boldsymbol{\lambda} \succ \mathbf{0}$ and solve the following scalar optimization

$$\begin{aligned} & \text{minimize } && \boldsymbol{\lambda}^T \mathbf{p} \\ & \text{subject to } && \mathbf{A}(\boldsymbol{\gamma})\mathbf{p} \succeq \mathbf{b}(\boldsymbol{\gamma}), \end{aligned} \quad (\text{A.4})$$

where the variable is \mathbf{p} . Let us make the change of variable $\mathbf{y} = \mathbf{A}(\boldsymbol{\gamma})\mathbf{p}$ and rewrite (A.4) as

$$\begin{aligned} & \text{minimize } && \boldsymbol{\lambda}^T \mathbf{A}(\boldsymbol{\gamma})^{-1} \mathbf{y} \\ & \text{subject to } && \mathbf{y} \succeq \mathbf{b}(\boldsymbol{\gamma}), \end{aligned} \quad (\text{A.5})$$

where the new variable is \mathbf{y} . Recall that $\mathbf{A}^{-1}(\boldsymbol{\gamma}) \succeq \mathbf{0}$ (since $\rho(\mathbf{B}(\boldsymbol{\gamma})\mathbf{G}) < 1$), and therefore the gradient of the objective has positive entries, i.e., $(\mathbf{A}(\boldsymbol{\gamma})^{-1})^T \boldsymbol{\lambda} \succeq \mathbf{0}$. Thus, the optimal solution does not depends on $\boldsymbol{\lambda}$ and it is given by $\mathbf{y}^* = \mathbf{b}(\boldsymbol{\gamma})$. This, in turn, implies that the optimal solution of (A.4) [and, implicitly of (A.3)] is given by $\mathbf{p}^* = \mathbf{A}^{-1}(\boldsymbol{\gamma})\mathbf{b}(\boldsymbol{\gamma})$.

APPENDIX B
COMPUTE $\boldsymbol{\gamma}_{\text{ImpCGP}}$ VIA COMPLEMENTARY
GEOMETRIC PROGRAMMING (CGP)

We show in the sequel how to compute efficiently $\boldsymbol{\gamma}_{\text{ImpCGP}}$ via CGP [53], when $f_0(\boldsymbol{\gamma}) = \sum_{l \in \mathcal{L}} -\beta_l \log(1 + \gamma_l)$.²¹ We start by equivalently reformulating (47) as

$$\begin{aligned} & \text{minimize } && \prod_{l \in \mathcal{L}} (1 + \gamma_l)^{-\beta_l} \\ & \text{subject to } && \gamma_{l,\min} \leq \gamma_l \leq \gamma_{l,\max}, l \in \mathcal{L} \\ & && \gamma_l \leq \frac{g_{ll} p_l}{\sigma^2 + \sum_{j \neq l} g_{jl} p_j}, l \in \mathcal{L} \\ & && \sum_{l \in \mathcal{O}(n)} p_l \leq p_n^{\max}, n \in \mathcal{T} \\ & && p_l \geq 0, l \in \mathcal{L}, \end{aligned} \quad (\text{B.1})$$

where the variables are $\{p_l, \gamma_l\}_{l \in \mathcal{L}}$. The equivalence between (47) and (B.1) follows from the monotonically increasing property of $\log(\cdot)$ function and the explicit description of the constraints. For the local minimization we slightly modified the solution method proposed in [52, Algorithm 2] as follows.

Algorithm 3: CGP Based Algorithm for Finding $\boldsymbol{\gamma}_{\text{ImpCGP}}$

- 1) Given tolerance $\varepsilon > 0$. Let $\hat{\boldsymbol{\gamma}} = \bar{\mathbf{a}}_{l^*}$.
- 2) Solve the following GP

$$\begin{aligned} & \text{minimize } && \prod_{l \in \mathcal{L}} \gamma_l^{-\beta_l \frac{\gamma_l}{1+\gamma_l}} \\ & \text{subject to } && \gamma_{l,\min} \leq \gamma_l \leq \gamma_{l,\max}, l \in \mathcal{L} \end{aligned}$$

²¹Note that this is the only place where the exact expression of the rate function (1) has been explicitly taken into account. In the derivation of all other bound only the monotonicity property has been used.

$$\gamma_l \leq \frac{g_l p_l}{\sigma^2 + \sum_{j \neq l} g_j p_j}, l \in \mathcal{L}$$

$$\sum_{l \in \mathcal{O}(n)} p_l \leq p_n^{\max}, n \in \mathcal{T} \quad (\text{B.2})$$

with the variables $\{p_l, \gamma_l\}_{l \in \mathcal{L}}$. Denote the solution by $\{p_l^*, \gamma_l^*\}_{l \in \mathcal{L}}$.

- 3) If $\max_{l \in \mathcal{L}} |\gamma_l^* - \hat{\gamma}_l| > \varepsilon$ set $\{\hat{\gamma}_l = \gamma_l^*\}_{l \in \mathcal{L}}$ and go to Step 2; otherwise set $\gamma_{\text{ImpCGP}} = \hat{\gamma}$ and STOP.

ACKNOWLEDGMENT

The authors would like to thank the anonymous reviewers for their comments which have improved the presentation and the quality of the paper.

REFERENCES

- [1] R. Nelson and L. Kleinrock, "Spatial TDMA: Collision-free multihop channel access protocol," *IEEE Trans. Commun.*, vol. 33, no. 9, pp. 934–944, Sep. 1985.
- [2] D. Tse and P. Viswanath, *Fundamentals of Wireless Communication*. Cambridge, U.K.: Cambridge Univ. Press, 2005.
- [3] T. Starr, M. Sorbara, J. Cioffi, and P. J. Silverman, *DSL Advances*. Upper Saddle River, NJ: Prentice-Hall, 2003.
- [4] Z. Q. Luo and W. Yu, "An introduction to convex optimization for communications and signal processing," *IEEE J. Sel. Areas Commun.*, vol. 24, no. 8, pp. 1426–1438, Aug. 2006.
- [5] R. Cendrillon, W. Yu, M. Moonen, J. Verlinden, and T. Bostoen, "Optimal multiuser spectrum balancing for digital subscriber lines," *IEEE Trans. Commun.*, vol. 54, no. 5, pp. 922–933, May 2006.
- [6] Y. Xu, S. Panigrahi, and T. Le-Ngoc, "A concave minimization approach to dynamic spectrum management for digital subscriber lines," in *Proc. IEEE Int. Conf. Commun.*, Istanbul, Turkey, Jun. 11–15, 2006, pp. 84–89.
- [7] Y. Xu, T. Le-Ngoc, and S. Panigrahi, "Global concave minimization for optimal spectrum balancing in multi-user DSL networks," *IEEE Trans. Signal Process.*, vol. 56, no. 7, pp. 2875–2885, Jul. 2008.
- [8] K. Eriksson, "Dynamic Resource Allocation in Wireless Networks," Examensarbete Utfört i Kommunikationssystem vid Tekniska Högskolan i Linköping 2010 [Online]. Available: <http://liu.diva-portal.org/smash/get/diva2:326290/FULLTEXT01>
- [9] H. Al-Shatri and T. Weber, "Optimizing power allocation in interference channels using D.C. programming," in *Proc. Workshop on Resource Allocat. in Wireless Netw.*, Avignon, France, Jun. 4, 2010, pp. 367–373.
- [10] P. Tsiaflakis, J. Vangorp, M. Moonen, and J. Verlinden, "A low complexity optimal spectrum balancing algorithm for digital subscriber lines," *Elsevier Signal Process.*, vol. 87, no. 7, Jul. 2007.
- [11] P. Tsiaflakis, W. Tan, Y. Yi, M. Chiang, and M. Moonen, "Optimality certificate of dynamic spectrum management in multi-carrier interference channels," in *Proc. IEEE Int. Symp. Inf. Theory*, Toronto, Canada, Jul. 6–11, 2008, pp. 1298–1302.
- [12] L. Qian, Y. J. A. Zhang, and J. Huang, "MAPEL: Achieving global optimality for a non-convex wireless power control problem," *IEEE Trans. Wireless Commun.*, vol. 8, no. 3, pp. 1553–1563, Mar. 2009.
- [13] R. Cendrillon, J. Huang, M. Chiang, and M. Moonen, "Autonomous spectrum balancing for digital subscriber lines," *IEEE Trans. Signal Process.*, vol. 55, no. 8, pp. 4241–4257, Aug. 2007.
- [14] P. Tsiaflakis, M. Diehl, and M. Moonen, "Distributed spectrum management algorithms for multiuser DSL networks," *IEEE Trans. Signal Process.*, vol. 56, no. 10, pp. 4825–4843, Oct. 2008.
- [15] R. Lui and W. Yu, "Low-complexity near-optimal spectrum balancing for digital subscriber lines," in *Proc. IEEE Int. Conf. Commun.*, Seoul, Korea, May 16–20, 2005, pp. 1947–1951.
- [16] J. Papandriopoulos and S. Evans, "Low-complexity distributed algorithms for spectrum balancing in multi-user DSL networks," in *IEEE Int. Conf. Commun.*, Istanbul, Turkey, Jun. 11–15, 2006, pp. 3270–3275.
- [17] L. Tassiulas and A. Ephremides, "Stability properties of constrained queueing systems and scheduling policies for maximum throughput in multihop radio networks," *IEEE Trans. Autom. Control*, vol. 37, no. 12, pp. 1936–1949, Dec. 1992.
- [18] L. Tassiulas and A. Ephremides, "Dynamic server allocation to parallel queues with randomly varying connectivity," *IEEE Trans. Inf. Theory*, vol. 39, no. 2, pp. 466–478, Mar. 1993.
- [19] A. Eryilmaz, R. Srikant, and J. R. Perkins, "Stable scheduling policies for fading wireless channels," *IEEE/ACM Trans. Netw.*, vol. 13, no. 2, pp. 411–424, Apr. 2005.
- [20] X. Wu and R. Srikant, "Regulated maximal matching: A distributed scheduling algorithm for multi-hop wireless networks with node-exclusive spectrum sharing," in *Proc. IEEE Conf. on Decision and Control Eur. Control Conf.*, Seville, Spain, Dec. 12–15, 2005, pp. 5342–5347.
- [21] M. J. Neely, E. Modiano, and C. E. Rohrs, "Power allocation and routing in multibeam satellites with time-varying channels," *IEEE/ACM Trans. Netw.*, vol. 11, no. 1, pp. 138–152, Feb. 2003.
- [22] X. Lin and N. B. Shroff, "Joint rate control and scheduling in multihop wireless networks," Purdue Univ., West Lafayette, IN, Tech. Rep., 2004 [Online]. Available: <http://cobweb.ecn.purdue.edu/linux/papers.html>
- [23] X. Lin and N. B. Shroff, "Joint rate control and scheduling in multihop wireless networks," in *Proc. IEEE Int. Conf. Decision Control*, Atlantis, Paradise Island, Bahamas, Dec. 14–17, 2004, vol. 5, pp. 1484–1489.
- [24] M. J. Neely, E. Modiano, and C. E. Rohrs, "Dynamic power allocation and routing for time varying wireless networks," *IEEE J. Sel. Areas Commun.*, vol. 23, no. 1, pp. 89–103, Jan. 2005.
- [25] X. Lin and N. B. Shroff, "The impact of imperfect scheduling on cross-layer rate control in wireless networks," in *Proc. IEEE INFOCOM*, Miami, FL, Mar. 13–17, 2005, vol. 3, pp. 1804–1814.
- [26] G. Sharma, R. R. Mazumdar, and N. B. Shroff, "On the complexity of scheduling in wireless networks," in *Proc. ACM Int. Conf. Mobile Comput. Netw.*, Los Angeles, CA, Sep. 24–29, 2006, pp. 227–238.
- [27] C. H. Papadimitriou and K. Steiglitz, *Combinatorial Optimization: Algorithms and Complexity*. Englewood Cliffs, NJ: Prentice-Hall, 1982.
- [28] M. J. Neely, "Super-fast delay tradeoffs for utility optimal fair scheduling in wireless networks," *IEEE J. Sel. Areas Commun.*, vol. 24, no. 8, pp. 1–12, Aug. 2006.
- [29] X. Lin, N. B. Shroff, and R. Srikant, "A tutorial on cross-layer optimization in wireless networks," *IEEE J. Sel. Areas Commun.*, vol. 24, no. 8, pp. 1452–1463, Aug. 2006.
- [30] L. Georgiadis, M. J. Neely, and L. Tassiulas, "Resource allocation and cross-layer control in wireless networks," *Found. Trends in Netw.*, vol. 1, no. 1, pp. 1–144, Apr. 2006.
- [31] M. J. Neely, E. Modiano, and C. Li, "Fairness and optimal stochastic control for heterogeneous networks," *IEEE/ACM Trans. Netw.*, vol. 16, no. 2, pp. 396–409, Apr. 2008.
- [32] Y. Yi and M. Chiang, "Stochastic network utility maximization: A tribute to Kelly's paper published in this journal a decade ago," *Eur. Trans. Telecommun.*, vol. 19, no. 4, pp. 421–442, Jun. 2008.
- [33] D. P. Palomar and M. Chiang, "Alternative distributed algorithms for network utility maximization: Framework and applications," *IEEE Trans. Autom. Control*, vol. 52, no. 12, pp. 2254–2269, Dec. 2007.
- [34] M. Chiang and J. Bell, "Balancing supply and demand of bandwidth in wireless cellular networks: Utility maximization over powers and rates," in *Proc. IEEE INFOCOM*, Hong Kong, Mar. 7–11, 2004, vol. 4, pp. 2800–2811.
- [35] M. Chiang, "Balancing transport and physical layers in wireless multihop networks: Jointly optimal congestion control and power control," *IEEE J. Sel. Areas Commun.*, vol. 23, no. 1, pp. 104–116, Jan. 2005.
- [36] A. Pantelidou and A. Ephremides, "A cross-layer view of wireless multicasting under uncertainty," in *Proc. IEEE Inf. Theory Workshop*, Volos, Greece, Jun. 10–12, 2009, pp. 110–114.
- [37] M. Codreanu, A. Tolli, M. Juntti, and M. Latva-aho, "Joint design of Tx-Rx beamformers in MIMO downlink channel," *IEEE Trans. Signal Process.*, vol. 55, no. 9, pp. 4639–4655, Sep. 2007.
- [38] R. Agarwal and J. M. Cioffi, "Beamforming design for the MIMO downlink for maximizing weighted sum-rate," in *Proc. IEEE Int. Symp. Inf. Theory and Its Appl.*, Auckland, New Zealand, Dec. 7–10, 2008, pp. 1–6.
- [39] L. Zhang, Y. Xin, Y. C. Liang, and H. V. Poor, "Cognitive multiple access channels: Optimal power allocation for weighted sum rate maximization," *IEEE Trans. Commun.*, vol. 57, no. 9, pp. 2754–2762, Sep. 2009.

- [40] A. Tölli, M. Codreanu, and M. Juntti, "Cooperative MIMO-OFDM cellular system with soft handover between distributed base station antennas," *IEEE Trans. Wireless Commun.*, vol. 7, no. 4, pp. 1428–1440, Apr. 2008.
- [41] C. Guthy, W. Utschick, R. Hunger, and M. Joham, "Efficient weighted sum rate maximization with linear precoding," *IEEE Trans. Signal Process.*, vol. 58, no. 4, pp. 2284–2297, Apr. 2010.
- [42] M. Stojnic, H. Vikalo, and B. Hassibi, "Rate maximization in multi-antenna broadcast channels with linear preprocessing," *IEEE Trans. Wireless Commun.*, vol. 5, no. 9, pp. 2338–2342, Sep. 2006.
- [43] S. S. Christensen, R. Agarwal, E. Carvalho, and J. Cioffi, "Weighted sum-rate maximization using weighted MMSE for MIMO-BC beamforming design," *IEEE Trans. Wireless Commun.*, vol. 7, no. 12, pp. 4792–4799, Dec. 2008.
- [44] S. Shi, M. Schubert, and H. Boche, "Weighted sum-rate optimization for multiuser MIMO systems," in *Proc. Conf. Inf. Sci. Syst. (CISS)*, Baltimore, MD, Mar. 14–16, 2007, pp. 425–430.
- [45] N. Vucic, S. Shi, and M. Schubert, "DC programming approach for resource allocation in wireless networks," in *Proc. Workshop on Resource Allocat. in Wireless Netw.*, Avignon, France, Jun. 4, 2010, pp. 360–366.
- [46] Z. Luo and S. Zhang, "Dynamic spectrum management: Complexity and duality," *IEEE J. Sel. Areas Commun.*, vol. 2, no. 1, pp. 57–73, Feb. 2008.
- [47] R. Horst, P. Pardalos, and N. Thoai, *Introduction to Global Optimization*, 2nd ed. Norwell, MA: Kluwer Academic, 2000, vol. 48.
- [48] *Essays and Surveys in Global Optimization*, C. Audet, P. Hansen, and G. Savard, Eds. New York: Springer Science + Business Media, 2005.
- [49] S. Boyd, Branch-and-Bound Methods, 2007 [Online]. Available: http://www.stanford.edu/class/ee364b/lectures/bb_slides.pdf
- [50] N. T. H. Phuong and H. Tuy, *A Unified Monotonic Approach to Generalized Linear Fractional Programming*. Boston, MA: Kluwer Academic, 2003, pp. 229–259.
- [51] S. Boyd and L. Vandenberghe, Additional Exercises for Convex Optimization, May 2010 [Online]. Available: http://www.stanford.edu/~boyd/cvxbook/bv_cvxbook_extra_exercises.pdf
- [52] M. Codreanu, P. C. Weeraddana, and M. Latva-aho, "Cross-layer utility maximization subject to stability constraints for multi-channel wireless networks," in *Proc. Ann. Asilomar Conf. Signals, Syst., Comput.*, Pacific Grove, CA, Nov. 2–4, 2009, pp. 776–780.
- [53] M. Avriel and A. C. Williams, "Complementary geometric programming," *SIAM J. Appl. Math.*, vol. 19, no. 1, pp. 125–141, Jul. 1970.
- [54] S. Boyd, S. J. Kim, L. Vandenberghe, and A. Hassibi, "A tutorial on geometric programming," *Opt. and Eng.*, vol. 8, no. 1, pp. 67–127, 2007.
- [55] M. Chiang, "Geometric programming for communication systems," *Found. Trends in Commun. Inf. Theory*, vol. 2, no. 1-2, pp. 1–154, Jul. 2005.
- [56] M. Cao, X. Wang, S. Kim, and M. Madhian, "Multi-hop wireless backhaul networks: A cross-layer design paradigm," *IEEE J. Sel. Areas Commun.*, vol. 25, no. 4, pp. 738–748, May 2007.
- [57] M. Kodialam and T. Nandagopal, "Characterizing achievable rates in multi-hop wireless mesh networks with orthogonal channels," *IEEE/ACM Trans. Netw.*, vol. 13, no. 4, pp. 868–880, Aug. 2005.
- [58] Y. Shi and Y. T. Hou, "A distributed optimization algorithm for multi-hop cognitive radio networks," in *Proc. IEEE INFOCOM*, Phoenix, AZ, Apr. 13–18, 2008, pp. 1292–1300.
- [59] M. Cao, V. Raghunathan, S. Hanly, V. Sharma, and P. R. Kumar, "Power control and transmission scheduling for network utility maximization in wireless networks," in *Proc. IEEE Int. Conf. Decision Control*, New Orleans, LA, Dec. 12–14, 2007, pp. 5215–5221.
- [60] D. E. Barreto and S. S. Chiu, "Decomposition methods for cross-layer optimization in wireless networks," in *Proc. IEEE Wireless Commun. Netw. Conf.*, Kawloon, Hong Kong, Mar. 11–15, 2007, pp. 270–275.
- [61] H. Suzuki, K. Itoh, Y. Ebin, and M. Sato, "A booster configuration with adaptive reduction of transmitter-receiver antenna coupling for pager systems," in *Proc. IEEE Veh. Technol. Conf.*, Amsterdam, The Netherlands, Sep. 19–22, 1999, vol. 3, pp. 1516–1520.
- [62] D. Halperin, T. Anderson, and D. Wetherall, "Taking the sting out of carrier sense: Interference cancellation for wireless LANs," in *Proc. ACM Int. Conf. on Mobile Comput. Netw.*, San Francisco, CA, Sep. 14–19, 2008, pp. 339–350.
- [63] B. Radunovic, D. Gunawardena, A. Proutiere, N. Singh, V. Balan, and P. Key, "Efficiency and fairness in distributed wireless networks through self-interference cancellation and scheduling," Tech. Rep. MSR-TR-2009-27, Microsoft Res., 2009 [Online]. Available: <http://research.microsoft.com/apps/pubs/default.aspx?id=79933>
- [64] B. Radunovic, D. Gunawardena, P. Key, A. Proutiere, N. Singh, V. Balan, and G. Dejean, "Rethinking indoor wireless: Low power, low frequency, full-duplex," Tech. Rep. MSR-TR-2009-148, Microsoft Research, 2009 [Online]. Available: <http://research.microsoft.com/apps/pubs/default.aspx?id=104950>
- [65] V. Balakrishnan, S. Boyd, and S. Balemli, "Branch and bound algorithm for computing the minimum stability degree of parameter-dependent linear systems," *Int. J. Robust and Nonlin. Control*, vol. 1, no. 4, pp. 295–317, Oct. 1991.
- [66] S. Boyd and L. Vandenberghe, *Convex Optimization*. Cambridge, U.K.: Cambridge Univ. Press, 2004.
- [67] B. Song, R. L. Cruz, and B. D. Rao, "Network duality and its application to multi-user MIMO wireless networks with SINR constraints," in *Proc. IEEE Int. Conf. Commun.*, Seoul, Korea, May 16–20, 2005, vol. 4, pp. 2684–2689.
- [68] R. A. Horn and C. R. Johnson, *Topics in Matrix Analysis*. Cambridge, U.K.: Cambridge Univ. Press, 1994.
- [69] S. Boyd, GGPLAB: A Simple Matlab Toolbox for Geometric Programming, 2006 [Online]. Available: <http://www.stanford.edu/boyd/ggplab/>
- [70] A. Kumar, D. Manjunath, and J. Kuri, *Wireless Networking*. Burlington, MA: Elsevier, 2008.
- [71] I. C. Abou-Faycal, M. D. Trott, and S. Shamai, "The capacity of discrete-time memoryless Rayleigh-fading channels," *IEEE Trans. Inf. Theory*, vol. 47, no. 4, pp. 1290–1301, May 2001.
- [72] H. Weingarten, Y. Steinberg, and S. Shamai, "The capacity region of the gaussian multiple-input multiple-output broadcast channel," *IEEE Trans. Inf. Theory*, vol. 52, no. 9, pp. 3936–3964, Sep. 2006.
- [73] D. N. Tse and S. V. Hanly, "Multiaccess fading channels-part I: Polymatroid structure, optimal resource allocation and throughput capacities," *IEEE Trans. Inf. Theory*, vol. 44, no. 7, pp. 2796–2815, Nov. 1998.
- [74] T. M. Cover and J. A. Thomas, *Elements of Information Theory*, second ed. New York: Wiley, 2006.
- [75] S. V. Hanly and D. N. Tse, "Multiaccess fading channels-part II: Delay limited capacities," *IEEE Trans. Inf. Theory*, vol. 44, no. 7, pp. 2816–2831, Nov. 1998.
- [76] J. Zander, "Performance of optimum transmitter power control in cellular radio systems," *IEEE Trans. Veh. Technol.*, vol. 41, no. 1, pp. 57–62, Feb. 1992.
- [77] G. J. Foschini and Z. Miljanic, "A simple distributed autonomous power control algorithm and its convergence," *IEEE Trans. Veh. Technol.*, vol. 42, no. 4, pp. 641–646, Nov. 1993.
- [78] R. D. Yates and C. Huang, "Integrated power control and base station assignment," *IEEE Trans. Veh. Technol.*, vol. 44, no. 3, pp. 638–644, Aug. 1995.
- [79] S. V. Hanly, "An algorithm for combined cell-site selection and power control to maximize cellular spread spectrum capacity," *IEEE J. Sel. Areas Commun.*, vol. 13, no. 7, pp. 1332–1340, Sep. 1995.
- [80] E. Seneta, *Non-Negative Matrices and Markov Chains*. New York: Springer Science + Business Media, 2006.



Pradeep Chathuranga Weeraddana (S'08) received the B.Sc. degree in electronic and telecommunication engineering with first class honors from the University of Moratuwa, Moratuwa, Sri Lanka, in 2004, and the M.Eng. degree telecommunication from the School of Engineering and Technology, Asian Institute of Technology, Thailand, in 2007.

He is currently working toward the Ph.D. degree with the Centre for Wireless Communications, Department of Electrical Engineering, University of Oulu, Finland. His research interests include

application of optimization techniques for signal processing and wireless communications.



Marian Codreanu (S'02–M'07) received the M.S. degree from the University Politehnica of Bucharest, Romania, in 1998, and the Ph.D. degree from the University of Oulu, Finland, in 2007.

From 1998 to 2002, he was Teaching Assistant with the Telecommunications Department, University Politehnica of Bucharest. In 2002, he joined the Centre for Wireless Communications (CWC), University of Oulu, where he currently holds a Senior Research Fellow position. In 2008, he was a Visiting Postdoctoral Researcher with the University of Maryland, College Park. His research interests include optimization, information theory, and signal processing for wireless communication systems and networks.

Dr. Codreanu received the Best Doctoral Thesis prize within the area of all technical sciences in Finland in 2007. He was a Co-Chair of the Technical Program Committee (TPC) of The First Nordic Workshop on Cross-Layer Optimization in Wireless Networks in 2010 and a Co-Chair of The Second Nordic Workshop on System and Network Optimization for Wireless (SNOW 2011).



Matti Latva-aho (S'96–M'98–SM'06) was born in Kuivaniemi, Finland, in 1968. He received the M.Sc., Lic.Tech., and Dr. Tech (Hons.) degrees in electrical engineering from the University of Oulu, Finland, in 1992, 1996, and 1998, respectively.

From 1992 to 1993, he was a Research Engineer with Nokia Mobile Phones, Oulu. During 1994–1998, he was a Research Scientist with Telecommunication Laboratory and Centre for Wireless Communications, University of Oulu. Currently, he is the Head of Telecommunication Laboratory

and Professor of Digital Transmission Techniques, University of Oulu. His research interests are related to mobile broadband wireless communication systems. He has published 200 conference or journal papers in the field of wireless communications.

Prof. Latva-aho was Director of the Centre for Wireless Communications, University of Oulu, during 1998–2006.



Anthony Ephremides (S'68–M'71–SM'77–F'84) received the Ph.D. degree in electrical engineering from Princeton University, Princeton, NJ, in 1971.

He has been with the University of Maryland ever since receiving his degree and holds the Cynthia Kim Professorship of Information Technology at the Electrical and Computer Engineering Department, University of Maryland in College Park. He also holds a joint appointment at the Institute for Systems Research, of which he was among the founding members in 1986. He has held various visiting positions at other Institutions (including MIT, UC Berkeley, ETH Zurich, INRIA, etc.) and cofounded and codirected a NASA-funded Center on Satellite and Hybrid Communication Networks in 1991. He is the author of several hundred papers, conference presentations, and patents, and his research interests lie in the areas of communication systems and networks and all related disciplines, such as information theory, control and optimization, satellite systems, queueing models, and signal processing. He is especially interested in wireless networks and energy efficient systems. He has been the President of Pontos, Inc., since 1980.

Dr. Ephremides served as President of the IEEE Information Theory Society in 1987 and was a member of the IEEE Board of Directors in 1989 and 1990. He has been the General Chair and/or the Technical Program Chair of several technical conferences, including the IEEE Information Theory Symposium in 1991, 2000, and 2011, the IEEE Conference on Decision and Control in 1986, the ACM Mobihoc in 2003, and the IEEE Infocom in 1999. He has served on the Editorial Board of numerous journals and was the Founding Director of the Fairchild Scholars and Doctoral Fellows Program, a University-Industry Partnership from 1981 to 1985. He received the IEEE Donald E. Fink Prize Paper Award in 1991 and the first ACM Achievement Award for Contributions to Wireless Networking in 1996, as well as the 2000 Fred W. Ellersick MILCOM Best Paper Award, the IEEE Third Millennium Medal, the 2000 Outstanding Systems Engineering Faculty Award from the Institute for Systems Research, and the Kirwan Faculty Research and Scholarship Prize from the University of Maryland in 2001. He also received the 2006 Aaron Wyner Award for Exceptional Service and Leadership to the IEEE Information Theory Society.